ADVANCED FUNCTIONAL MATERIALS
www.afm-journal.de



# A Light-Curable and Tunable Extracellular Matrix Hydrogel for In Situ Suture-Free Corneal Repair

*Ghasem Yazdanpanah, Xiang Shen, Tara Nguyen, Khandaker N. Anwar, Oju Jeon, Yizhou Jiang, Mohammad Pachenari, Yayue Pan, Tolou Shokuhfar, Mark I. Rosenblatt, Eben Alsberg, and Ali R. Djalilian**

**Corneal injuries are a major cause of blindness worldwide. To restore corneal integrity and clarity, there is a need for regenerative biointegrating materials for in situ repair and replacement of corneal tissue. Here, light-curable cornea matrix (LC-COMatrix), a tunable material derived from decellularized porcine cornea extracellular matrix containing un-denatured collagen and sulfated glycosaminoglycans is introduced. It is a functionalized hydrogel with proper swelling behavior, biodegradation, and viscosity that can be cross-linked in situ with visible light, providing significantly enhanced biomechanical strength, stability, and adhesiveness. The cross-linked LC-COMatrix strongly adheres to human corneas ex vivo and effectively closes full-thickness corneal perforations with tissue loss. Likewise, in vivo, LC-COMatrix seals large corneal perforations, replaces partial-corneal stromal defects and biointegrates into the tissue in rabbit models. LC-COMatrix is a natural ready-to-apply biointegrating adhesive that is representative of native corneal matrix with potential applications in corneal and ocular surgeries.**

## 1. Introduction

Corneal injuries and scarring are a major cause of blindness worldwide. Currently, the most effective therapy for corneal blindness is corneal transplantation using cadaver tissue which is only available to less than 5% of patients, worldwide. Donor organ shortage, expensive and skill-based surgical procedures, and graft-rejection are major challenges of corneal transplantation.[1] Fabrication of intact decellularized corneas from xenogeneic sources has been pursued for more than a decade to overcome the donor cornea shortage obstacle,[2] however; this strategy has not shown promising results in clinical translation.[3] A novel approach to meet the clinical demand for cornea tissue replacement and wound closure is to develop in situ cross-linking biomaterials. Currently, none of the available tissue sealants in the market such as fibrin glue (e.g., VISTASEAL, TISSEEL), cyanoacrylate based bioglues (e.g., Histoacryl, DERMABOND), and polyethylene glycol (PEG)-based bioglues (ReSure, OcuSeal) are suitable as a pro-regenerative corneal stromal replacement, and could be applied only for temporary sealing of ocular penetrations.[4] Fibrin gels are limited by the lack of necessary biomechanical stability and time-consuming preparations,[5] cyanoacrylate is opaque and provides no opportunity for biointegration,[6] and the PEG-based products lack the stability and strength for application in larger corneal defects.[4]

Recently, several experimental products have been introduced for the in situ repair and/or replacement of the corneal stroma. These products are generally classified into two categories. The first category is in situ light-curable products that need to be cured with a light-source to initiate cross-linking such as gelatin-methacrylate (GelMA),[7] and thiol–acrylate gelatin.[8] The main advantages of light-curable products over chemically cross-linkable products are lack of preapplication preparation, and more control over the photo-cross-linking process. However, gelatin-based products are commonly denatured purified skin collagen, which is not representative of corneal tissue and has temperature dependent viscosity which limits their user-friendly application in clinical settings. The second group is in situ chemically cross-linkable products (e.g., fibrin-based and PEG-based materials).[9] These materials are commonly prepared by combining of two or three components and the cross-linking starts immediately. Limited control on cross-linking reaction and lack of proper biomechanical stability are the constraints of this category.

A novel approach for the in situ repair and regeneration of the cornea is to engineer biomaterials from decellularized

G. Yazdanpanah, X. Shen, T. Nguyen, K. N. Anwar, M. I. Rosenblatt, A. R. Djalilian
Department of Ophthalmology and Visual Sciences
Illinois Eye and Ear Infirmary
University of Illinois at Chicago
Chicago, IL 60612, USA
E-mail: adjalili@uic.edu

G. Yazdanpanah, O. Jeon, T. Shokuhfar, E. Alsberg, A. R. Djalilian
Department of Biomedical Engineering
University of Illinois at Chicago
Chicago, IL 60607, USA

Y. Jiang, M. Pachenari, Y. Pan
Department of Mechanical and Industrial Engineering
University of Illinois at Chicago
Chicago, IL 60607, USA

The ORCID identification number(s) for the author(s) of this article can be found under https://doi.org/10.1002/adfm.202113383.

**DOI: 10.1002/adfm.202113383**

 

corneal ECM containing a balanced composition of collagens, glycoproteins, and sulfated glycosaminoglycans (sGAGs) analogous to the native cornea.[10] Recent studies on biomaterials fabricated from other decellularized tissues have shown that they can not only be applied as tissue engineering scaffolds, but they also have regenerative effects compared to purified and denatured natural biomaterials.[10b,11] Moreover, it has been shown that porcine corneal matrix protein has the highest similarity to human corneal matrix protein across species.[12] Our group recently reported on a thermoresponsive hydrogel from decellularized porcine ECM, cornea matrix (COMatrix),[13] which is liquid at temperatures below 15 °C and irreversibly forms a gel at 37 °C. The fabricated thermoresponsive COMatrix is composed of various types of collagens as well as sulfated glycosaminoglycans and proteoglycans with wound healing effects including lumican, keratocan, and laminin.[13a] The exact mechanism of thermoresponsive behavior of the COMatrix hydrogel is not clear. However, it has been suggested that partially digested collagens are thermodynamically able to rebuild the structure at 37 °C.[14] Moreover, the presence of sGAGs in the fabricated biomaterial increase the complexity of thermogelation.[13,14] We have investigated the use of thermoresponsive COMatrix as an ocular surface bandage for enhancing the healing of corneal epithelial wounds.[13b] However, the thermoresponsive COMatrix, as well as all similar decellularized cornea-based hydrogels reported by others,[10a,c,15] lack the biomechanical properties and stability needed for the repair and/or replacement of corneal stromal defects. Many protocols for chemical cross-linking of decellularized ECM-based hydrogels lead to the loss of transparency (e.g., following genipin cross-linking) or induce high-levels of cytotoxicity.[16] Moreover, chemical cross-linking requires preapplication combination of biomaterial and cross-linker with limited control over the cross-linking process. Therefore, we set out to develop and optimize a protocol to functionalize our thermoresponsive COMatrix hydrogel to a light curable cornea matrix (LC-COMatrix), which after light curing achieves a biomechanical strength comparable to human cornea while maintaining its optical and biological effects (**Figure 1**). Here, we have compositionally and mechanically characterized LC-COMatrix and evaluated its adhesion strength compared to fibrin glue and GelMA ex vivo. Moreover, the biocompatibility and potential application of LC-COMatrix for the in vivo repair and replacement of full-thickness corneal stromal defects was evaluated in a rabbit model.

## 2. Results

### 2.1. Compositional and Physical Characterization of Light-Curable COMatrix Hydrogel

The previously reported thermoresponsive COMatrix hydrogels have the advantage of genuine resemblance to corneal tissue compared to other biomaterials like gelatin or fibrin;[13a] however, they are limited by the biomechanical characteristics (storage modulus ($G'$), 83.3 ± 4.2 Pa),[13a] which makes it unsuitable for corneal stromal repair or replacement without additional cross-linking. Thus, in pilot studies we evaluated multiple approaches, including photo and chemical based cross-linking methods, in order to achieve the necessary biomechanical properties without compromising transparency or leading to undue toxicity. Considering user-friendly preparation and application, potential for shelf storage, controllable cross-linking process, low toxicity, and preserved transparency of the final product, we found that among the various methods for functionalizing the thermoresponsive COMatrix, reacting with methacrylate anhydride (MA) was able to fabricate an LC-COMatrix hydrogel without loss of transparency (Figure 1). Visible light curing (preferred over UV-based photocuring systems) was enabled by combining LC-COMatrix with an FDA approved photoinitiating cocktail including eosin Y, triethanolamine (TEOA), and *N*-vinylcaprolactam (VC). Curing the prepared combination with green-light (520 nm, peak absorbance for eosin Y), begins the cross-linking reaction and stiffens the hydrogel.[7] LC-COMatrix hydrogel samples were prepared as ready-to-cure and loaded in syringes (Figure S1, Supporting Information) for further experiments.

To optimize the functionalization protocol, COMatrix was reacted with MA with different ratios including 2:1 (0.5×), 1:1 (1×), and 1:2 (2×). The degree of functionalization was measured with nuclear magnetic resonance (NMR) spectroscopy and fluoraldehyde assay. NMR spectroscopy showed the peaks for methacryloyl (methacrylate/methacrylamide) functional groups at 5.5 to 6 ppm compared to nonfunctionalized COMatrix (**Figure 2**A). As the ratio of MA to COMatrix increased, the methacrylate peaks became stronger indicating more attached methacrylate groups to the fabricated matrix. This was consistent with results from the fluoraldehyde assay, which measured the degree of functionalization (DoF) by quantifying the total number of free amine-groups (majority of methacrylate groups are attaching to free amine groups). With increasing ratio of MA:COMatrix from 1:2 to 1:1, and to 2:1, the number of free amine groups decreased while the DoF increased. The DoF was 12.7% ± 2.5%, for 0.5×, 40% ± 4.5% for 1×, and 70.3% ± 5.2% for 2× LC-COMatrix ($P < 0.0001$, ANOVA, $N = 4$, Figure 2B).

To evaluate whether the functionalization process influenced the general content of the COMatrix, the collagen and sulfated glycosaminoglycan compositions in COMatrix and variants of LC-COMatrix were measured and compared with human cadaver corneas and GelMA. Similar collagen and sGAG concentrations were found in all samples indicating that the MA functionalization had not significantly affected the general content of COMatrix and was comparable to human corneas. On the other hand, only collagen was detected in GelMA (Figure 2C,D).

Swelling of cornea is one of the major reasons for its decreased optical clarity (and visual acuity) after corneal repair or transplantation. Therefore, any potential biomaterial for corneal stromal repair needs to have negligible swelling while it is in an aqueous environment. Here, the water content of the cross-linked LC-COMatrix was measured while incubating in salt-balanced solution and compared with those of cross-linked fibrin glue, 20% GelMA, and cadaveric human cornea. The water content of COMatrix, GelMA, and fibrin gel was more than 95% compared to 85.7% ± 1.5% for human corneas. As presented in Figure 2E, human corneal buttons experienced a primary swelling of 3.3% ± 0.9% while the 2× LC-COMatrix had less than 1% change in water content for the first day. The

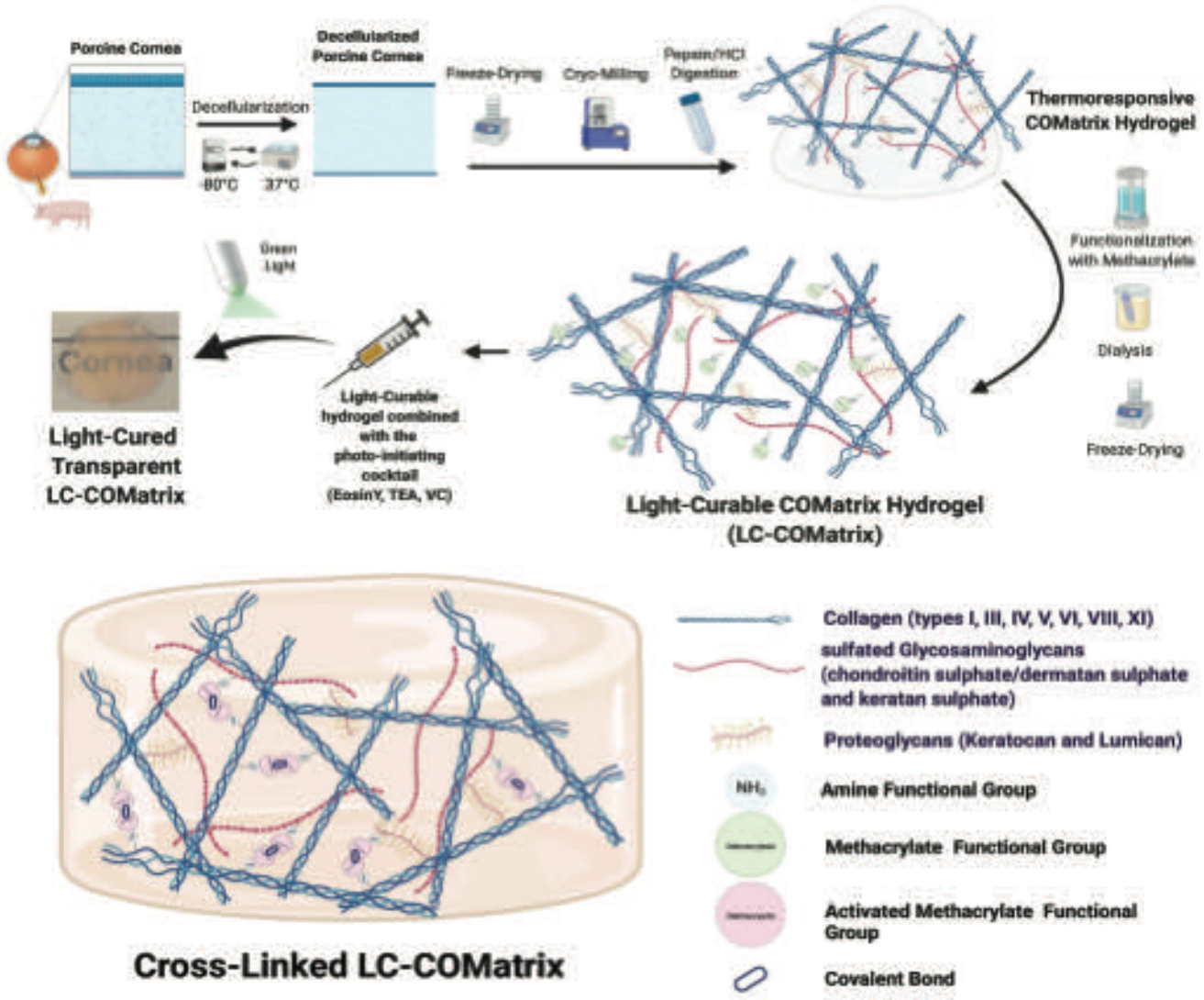


**Figure 1.** The fabrication process of light-curable COMatrix (LC-COMatrix) hydrogel. Porcine corneas were decellularized using freeze–thaw method and partially digested with pepsin/HCl cocktail to fabricate thermoresponsive COMatrix hydrogel.[13] To functionalize COMatrix into a light-curable substrate, the hydrogel has been reacted with methacrylate anhydride to connect methacrylate groups to the amine ($-NH_2$) functional groups on the collagens, sulfated glycosaminoglycans, and proteoglycans (the presence of these molecules in the COMatrix has already been shown by our group).[13a] Then, the fabricated light-curable COMatrix was combined with photoinitiating cocktail (including eosin Y, triethanolamine (TEA), and *N*-vinylcaprolactam (VC) to prepare the ready-to-cure hydrogel). The prepared LC-COMatrix could be cross-linked with visible green light with various times and durations. The photo-cross-linked LC-COMatrix hydrogel is transparent.

changes in the water contents of COMatrices, 20% GelMA, and human corneas were negligible during the 18 days of follow-up indicating no significant swelling or degradation. Interestingly, the fibrin gel lost water weight during the experiment indicating progressive degradation.

To simulate and evaluate the in vivo biodegradability of fabricated corneal matrix hydrogels compared to human corneas, the constructs/tissues were exposed to collagenase and intermittently weighed. Human corneas incubated in collagenase experienced an initial increase in weight due to swelling after which during the 10-day exposure to collagenase the weight decreased by 68.8% ± 5.3%. The degradation of LC-COMatrix samples was correlated with their DoF, with the 0.5× LC-COMatrix and 1× LC-COMatrix being 100% degraded after 10 days while the 2× LC-COMatrix was reduced by 90.4% ± 1.7% in weight at 10 days. The COMatrix (non-light-curable form), 20% GelMA, and fibrin glue were also found to be 100% degraded after 10 days but as shown in Figure 2F, their degradation rates were faster than LC-COMatrix.

### 2.2. Viscosity Characterization and Photogelation Kinetics of Light-Curable COMatrix

One of the challenges with the application of current bioadhesives in ophthalmology is the consistency of the bioadhesive at the time of application.[6] Specifically, the bioadhesive besides having strong adhesion after polymerization, requires

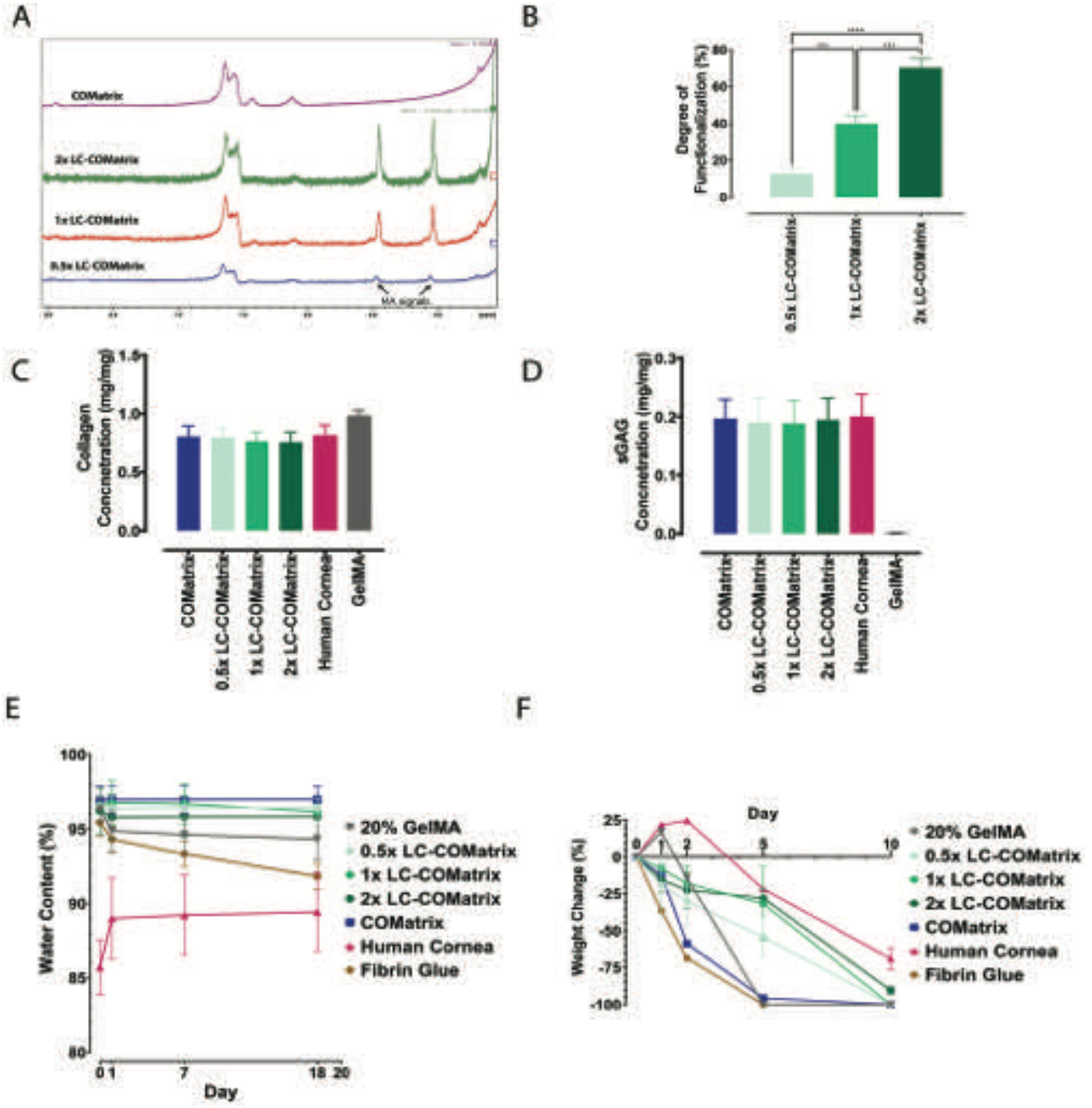


**Figure 2.** Biochemical and biophysical characterization of light-curable COMatrix hydrogel. A) NMR results of 0.5×, 1×, and 2× LC-COMatrices compared to thermoresponsive COMatrix. B) The degree of functionalization of 0.5×, 1×, and 2× LC-COMatrices measured by fluoraldehyde assay ($N = 4$, one-way ANOVA with Tukey post-test). C,D) The collagen and sGAG composition of light-curable and thermoresponsive COMatrices compared to human cornea and GelMA, respectively ($N = 4$). E) Changes in water content of COMatrix samples during incubation in PBS compared to human cornea, 20% GelMA, and fibrin glue. Two-way ANOVA statistical analysis with Tukey post-test multiple comparison of each material water content in each time point have not shown a significant difference ($N = 4$). F) Changes in weight of COMatrix disks incubated with collagenase compared to human cornea, 20% GelMA, and fibrin glue. Two-way ANOVA statistical analysis with Tukey post-test multiple comparison have not shown significant difference between 2× LC-COMatrix and human cornea weight change (%) in all time points ($N = 4$). ***, $P < 0.0001$; ****, $P < 0.00001$.

robust cohesion before cross-linking. If the bioadhesive has a low cohesion (very liquid) it will easily spread over the field to undesired areas before cross-linking, while if it is too viscous (very high cohesion), it will not adequately spread to provide coverage of the targeted area. For example, one of the main complaints of ophthalmologists who are using fibrin glue or cyanoacrylate on the corneal surface is the low cohesion of these products that leads to spreading on the surface to the

unwanted areas after application and before cross-linking. GelMA also has the same drawback, since at or below room temperatures it has strong cohesion but after warming to 37 °C the cohesion decreases significantly resulting in dispersal to surrounding areas.[17] One of the most common materials utilized in ophthalmology is a combination of sodium hyaluronate and chondroitin sulfate, so-called "Ophthalmic ViscoElastic Agent (ViscoElastic)," which has proper cohesion that provides necessary augmentation and protection in ophthalmic surgeries. The shear-thinning characteristics of OVA make it a suitable injectable material for in situ application. For the rheological characterizations of LC-COMatrix, we first measured the viscosity of 2× LC-COMatrix at 37, 25, and 12 °C by increasing the shear rate from 0.01 to 1000 ($S^{-1}$) and compared the results with a ViscoElastic, 20% GelMA, and the thicker component (fibrinogen) of fibrin glue (prior to combining with thrombin the thinner component) (**Figure 3**A–C). The viscosity of 2× LC-COMatrix was considerably higher than fibrin glue and 20% GelMA at 37 °C, which had minimal dependence on the temperature, thus, it would not be expected to spread excessively to undesired areas after application. Moreover, the 2× LC-COMatrix showed shear-thinning like the ViscoElastic Agent, which indicates its potential for injections or 3D-printing. On the other hand, 20% GelMA showed shear-thickening followed by shear-thinning by increasing in the shear rate at 25 and 12 °C (Figure 3A,B). The temperature dependent viscosity and shear-thickening behavior of GelMA at room temperature and lower temperatures has also been shown in previous studies,[17,18] which is not desirable for injection in clinical settings. This was the main reason that GelMA

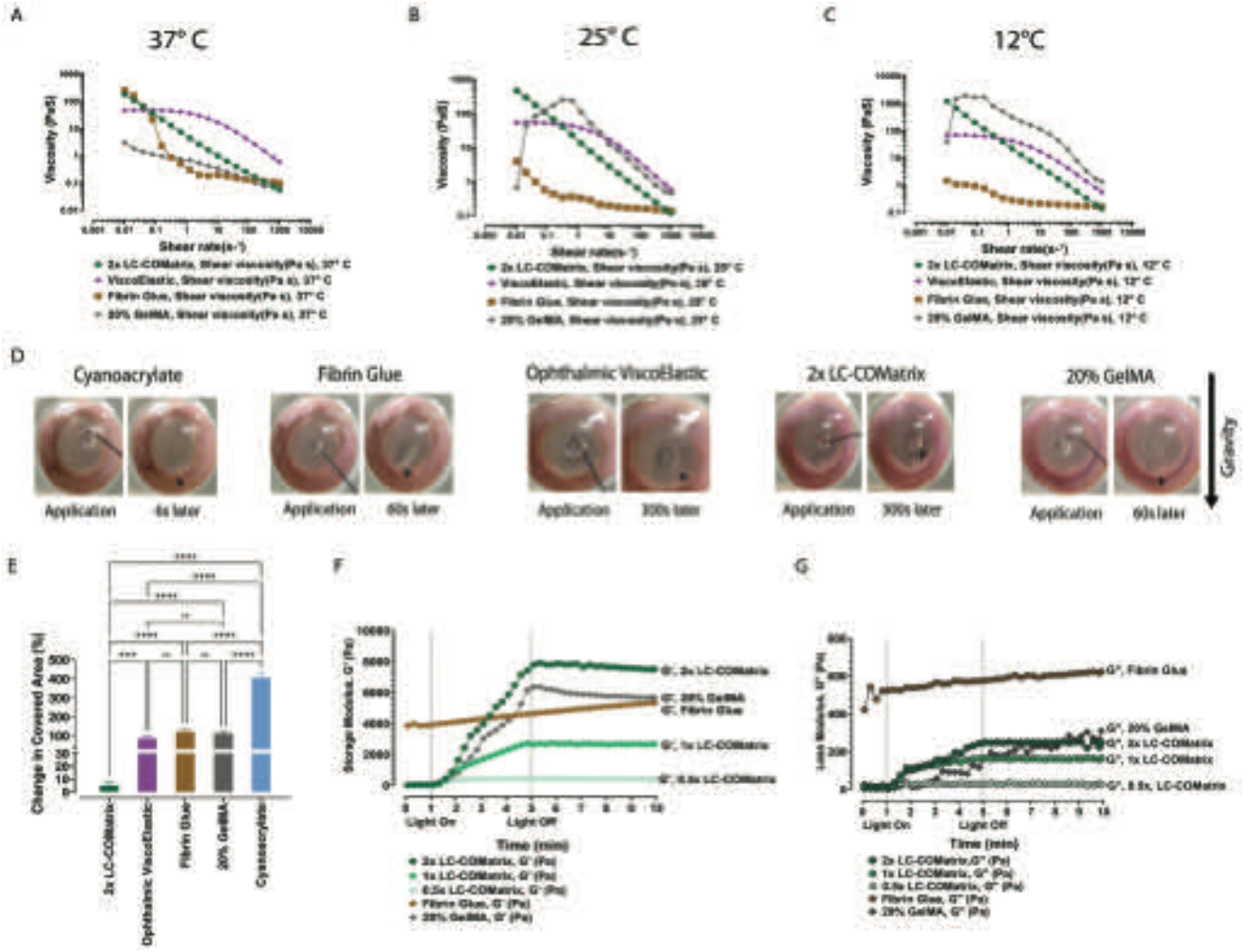


**Figure 3.** Rheological characterization of LC-COMatrix. Viscosity of 2× LC-COMatrix, ViscoElastic, fibrin glue, and 20% GelMA with shear rate change at A) 37 °C, B) 25 °C, and C) 12 °C ($N = 4$). D) Representative photos showing the effect of gravity on the behavior of adhesive materials (cyanoacrylate, fibrin glue, ViscoElastic, 20% GelMA, and 2× LC-COMatrix) while applied on the marked area (3 mm diameter) of cadaveric human corneas stabilized upright on a slit-lamp (see Videos S1–S5, Supporting Information). E) The change in covered area (%) following application of the bioadhesives on the upright cadaveric human corneas. The percentage of change in covered area was calculated by measuring the covered area immediately after application and 300 s later in the taken photos (see the Experimental Section, $N = 4$, one-way ANOVA with Tukey post-test). Recorded shear moduli (F) storage component, $G'$ and G) loss component, $G''$) of LC-COMatrix with different DoFs and 20% GelMA while curing with green light from minute 1 to minute 5 to record the gelatin kinetics of these hydrogels. The results were compared to recorded shear moduli of completely cross-linked fibrin glue ($N = 4$). ns, not significant; ***, $P < 0.0001$; ****, $P < 0.00001$.

was combined with hyaluronic acid or chitosan to tailor its viscosity,[19] while the LC-COMatrix does not need supplemental materials since it is a natural combination of collagen and sGAGs.[13a]

A descriptive experiment was performed to evaluate the behavior of LC-COMatrix compared to cyanoacrylate, fibrin glue, ViscoElastic, and 20% GelMA (37 °C) while applied to an ex vivo human cornea in an upright position. This experiment simulated the same position of the patient's eye in the ophthalmology clinic, where usually the bioadhesives are applied at a slit-lamp biomicroscope. As presented in Figure 3D, cyanoacrylate spread downward due to gravity in about 6 s. Fibrin glue and 20% GelMA were displaced downward in 60 s; while the ViscoElastic and LC-COMatrix remained stable in the applied area for 5 min, which provides sufficient time for light-curing. The videos of this experiment are available in Videos S1–S5 of the Supporting Information. Furthermore, a quantitative image analysis was performed to measure the area covered by each bioadhesive immediately after application and at 5 min follow-up and the change in covered area (%) was calculated ($N = 4$, Figure 3E). The changes in covered area by ophthalmic viscoelastic, fibrin glue, 20% GelMA, and cyanoacrylate after 5 min was 85.7% ± 11.3%, 120.4% ± 15.8%, 112.5% ± 9.7%, and 405.2% ± 27.3%, respectively. While the 2× LC-COMatrix covered area change was 5.1% ± 2.4% ($P < 0.001$ for LC-COMatrix compared to other bioadhesives, $N = 3$). Moreover, we evaluated whether the LC-COMatrix could be cured using the in-built green-light source of a slit-lamp biomicroscope (Video S6, Supporting Information). After 4 min of curing, the LC-COMatrix was strongly attached to a cadaveric human cornea mounted behind the slit-lamp (Video S7, Supporting Information).

To record the photogelation kinetics of LC-COMatrix and 20% GelMA by rheometry, the LC-COMatrices (0.5×, 1×, and 2×) were loaded onto the quartz glass surface of the rheometer with a green light source (100 μW $cm^{-2}$) installed below. The junction gap was set to be 0.4 mm and the shear moduli (storage, $G'$, **Figure 4**E; and loss, $G''$, Figure 4F) were recorded at 0.159 Hz frequency and 5% strain for 1 min. Then, the green light was turned on (Figure S2, Supporting Information) for 4 min while the recording continued. As plotted in Figure 3E,F, LC-COMatrix undergoes rapid photogelation during the first minute of curing with green light which then becomes more flattened and plateaued depending on the DoF. For 0.5× LC-COMatrix, the cross-linking finished after almost 1 min and the storage modulus did not increase. In case of 1× LC-COMatrix and 2× LC-COMatrix, more cross-linking occurred after the first minute surge evident by the increasing $G'$, but the slope of cross-linking was in accordance with the DoF. To measure the shear moduli of the fibrin glue, the two components were mixed and immediately loaded onto the rheometry plate and allowed to fully react for 30 min followed by recording at the same frequency and strain as above. The average $G'$ and $G''$ for photogelated 2× LC-COMatrix was 7.8 ± 0.5 and 0.2 ± 0.04 kPa, respectively, which was higher than fibrin glue with $G'$ of 4.8 ± 0.3 and $G''$ of 0.5 ± 0.07 kPa and 20% GelMA with $G'$ of 5.1 ± 3.2 kPa and $G''$ of 0.2 ± 0.16 kPa ($N = 3$, Figure 3E,F). The 1× LC-COMatrix and 0.5× LC-COMatrix had average $G'$ of 2.7 ± 0.5 and 0.4 ± 0.04 kPa, and average $G''$ of 0.2 ± 0.03 and 0.03 ± 0.007 kPa, respectively. Figure S2 of the Supporting Information presents a 2× LC-COMatrix sample after performing all the rheological tests while still preserving an intact structure.

### 2.3. Adhesion Strength of Light-Curable COMatrix on Ex Vivo Human Corneal Substrates

To measure the adhesion strength of LC-COMatrix, we conducted tensile adhesion tests using human corneas as the substrate. Human corneas were cut in half then fixed in the tensile testing grips with a 1 mm distance between the two halves (illustrated in **Figure 4**A and representative photos in Figure S3, Supporting Information). The half-corneas were glued with LC-COMatrix with various DoFs, 20% GelMA (followed by 4 min green light-curing), cyanoacrylate, or fibrin glue (3 mm width, $N = 6$ per group) and then subjected to tensile testing. The adhesion strength of 2× LC-COMatrix was 21.8 ± 2.3 kPa, which was significantly higher than that of 20% GelMA (11.1 ± 3.8 kPa, $p < 0.0001$), cyanoacrylate (10.7 ± 2.3 kPa), and fibrin glue (4.9 ± 2.3 kPa, $p < 0.0001$). The adhesion strength of 1× LC-COMatrix and 0.5× LC-COMatrix were 11.1 ± 3.7 and 3.6 ± 1.8 kPa, respectively (Figure 4B). In previous studies the adhesion strength of 20% GelMA after 4 min of light-curing was reported as 90.4 ± 10.2 kPa using a setup with porcine skin. Here, for the first time we have established a setup using cadaveric human corneas to measure the adhesion strength of the developed biomaterial which could justify the observed difference.[7] The adhesion strength tunability of LC-COMatrix provides the potential to fabricate the bioadhesive based on the targeted application.

### 2.4. Repair of Ex Vivo Penetrating Human Corneal Wounds with Light-Curable COMatrix

To test the wound integrity following the repair of corneal injuries, we mounted human cadaver corneas in an artificial anterior chamber and measured the burst pressure (BP) of the wounds after sealing with different LC-COMatrices, 20% GelMA, fibrin glue, or cyanoacrylate (Figure 4C). The created injuries were 2 and 1 mm full thickness punch wounds (the cut tissue was removed), and 2.75 and 5.90 mm full thickness stab wounds created by surgical knives. After drying the injury sites, LC-COMatrix with various DoFs or 20% GelMA were applied to the injury site (Figure 4D; Video S8, Supporting Information) and cured with green light for 4 min (Figure 4E). Figure 4F–I presents the photos of injuries before and after repair with 2× LC-COMatrix as well as the BP results for LC-COMatrices with various DoFs compared to 20% GelMA and fibrin glue ($N = 4$ per group). The average BP of the 2 mm punch injury repaired with 2× LC-COMatrix was 327 ± 175 mmHg (see Video S9, Supporting Information), while this value for 20% GelMA was 151 ± 48 mmHg ($p = 0.007$), for cyanoacrylate was 234 ± 145 ($p = 0.27$) and for fibrin glue was 11 ± 4 mmHg ($p < 0.0001$, Figure 4F). The LC-COMatrices with lower DoFs had lower burst pressures (1× LC-COMatrix BP, 240 ± 113 mmHg, and 0.5× LC-COMatrix BP, 151 ± 71 mmHg). The same pattern of results was seen with other types of penetrating corneal

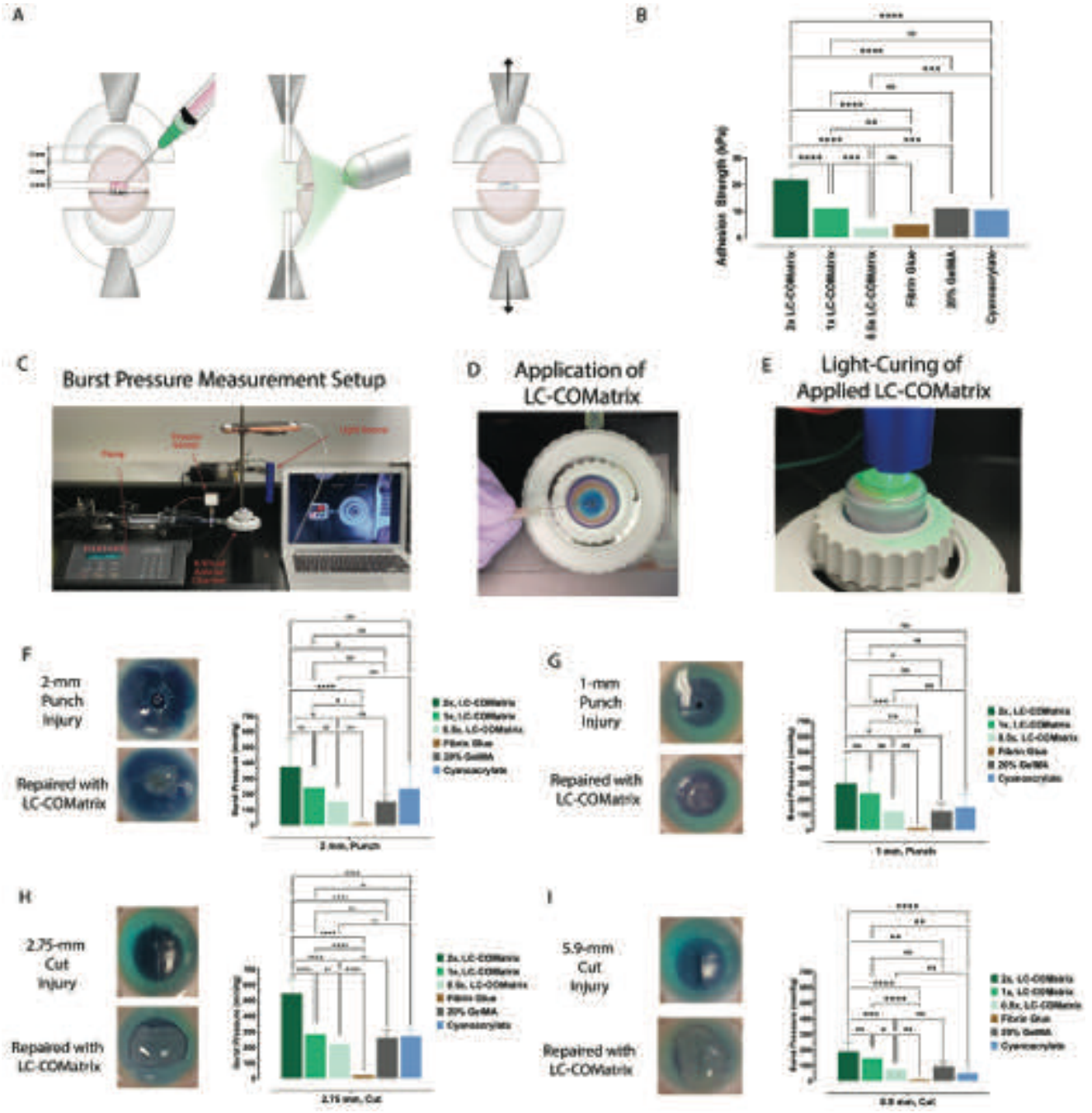


**Figure 4.** Adhesion strength of LC-COMatrix hydrogel and ex vivo repair of corneal penetrations and perforation with burst pressure measurement. A) Schematic illustration showing the setup and procedure for measuring the adhesion strength of LC-COMatrix, 20% GelMA, and fibrin glue on cadaveric human corneas (see representative photos in Figure S3, Supporting Information). B) The adhesion strength of LC-COMatrix with various DoFs compared to 20% GelMA, fibrin glue, and cyanoacrylate ($N = 6$). C) The setup for evaluating the wound closure capability of the LC-COMatrix and measuring the burst pressure. D) Applying the LC-COMatrix on human corneal model of full thickness wound (see Video S8, Supporting Information). E) Green light-curing of the applied hydrogel on the human cornea. F) 2 mm full thickness punch injury before and after repair (left) and the results of burst pressure tests for 0.5×, 1×, and 2× LC-COMatrix, fibrin glue, 20% GelMA, and cyanoacrylate (right, see Video S9, Supporting Information). G) 1 mm full thickness punch injury before and after repair (left) and the results of burst pressure tests for 0.5×, 1×, and 2× LC-COMatrix, fibrin glue, 20% GelMA, and cyanoacrylate (right, $N = 4$). H) 2.75 mm full thickness cut injury before and after repair (left) and the results of burst pressure tests for 0.5×, 1×, and 2× LC-COMatrix, fibrin glue, 20% GelMA, and cyanoacrylate (right, $N = 4$). I) 5.9 mm full thickness cut injury before and after repair (left) and the results of burst pressure tests for 0.5×, 1×, and 2× LC-COMatrix, 20% GelMA, fibrin glue, and cyanoacrylate (right). One-way ANOVA with Tukey post-test was performed for all comparisons in this figure. ns, not significant; *, $P < 0.05$; **, $P < 0.01$; ***, $P < 0.001$, ****, $P < 0.00001$.

injuries, where the BPs for 1 mm punch, 2.75 mm cut, and 5.9 cut repaired with 2× LC-COMatrix were 300 ± 160, 542 ± 86, and 188 ± 63 mmHg, respectively, compared to fibrin glue, which the BPs were 13 ± 2,19 ± 4, and 8 ± 4 mmHg, respectively ($p < 0.001$ for all comparisons). Again, as the DoF decreased in the fabricated COMatrices, lower BPs were recorded for each injury model (Figure 4F–I). Moreover, the recorded BPs for 1 mm punch, 2.75 mm cut, and 5.9 cut penetrating injuries repaired with cyanoacrylate were 150 ± 80 271 ± 43, and 48 ± 16 mmHg, respectively. The recorded BPs for 1 mm punch, 2.75 mm cut, and 5.9 cut penetrating injuries repaired with 20% GelMA were 124 ± 49, 259 ± 51, and 95 ± 33 mmHg, respectively. Since, 2× LC-COMatrix showed superior characteristics in the above experiments, it was used for further in vitro, ex vivo, and in vivo experiments.

### 2.5. Cytocompatibility of Light-Curable COMatrix Hydrogel In Vitro

Biomaterials applied for corneal repair should be biocompatible with the most abundant cell types in the cornea, namely, epithelial cells and stromal cells. Corneal epithelial cells typically grow over the surface while corneal stromal cells migrate into the applied biomaterial. The viability of human corneal epithelial cells (HCECs) and human corneal mesenchymal stem cells (hcMSCs) seeded on the cross-linked LC-COMatrix and thermogelated COMatrix was evaluated with a live–dead assay. As presented in Figure S4 of the Supporting Information, both HCECs and hcMSCs showed more than 95% viability in the construct. Evaluation of the number of viable cells at days 1, 4, 9, and 15 by metabolic assay revealed that both HCECs and hcMSCs had increased rate of proliferation until day 9, after which the cells went into steady growth from day 9 to day 15 on both COMatrix and LC-COMatrix (**Figure 5**B,D, Supporting Information).

One of the main concerns regarding the interaction of a biomaterial and mesenchymal stromal cells is their transdifferentiation into smooth muscle-like cells, specifically, myofibroblasts, which are the main mediators of corneal fibrosis/scarring.[20] To evaluate the effect of LC-COMatrix on myofibroblast formation, LC-COMatrix combined with hcMSCs was cured with green light after which the cross-linked hydrogel (containing the cells inside) was cultured for 2 weeks. After two weeks the hydrogel disks were stained for the expression of CD90, as a marker of hcMSCs, ki-67 marker, as a marker of cell proliferation, and $\alpha$-SMA ($\alpha$-smooth muscle actin), as a marker of myofibroblasts. Ki-67 marker was strongly expressed in the CD90 positive hcMSCs indicating active cell proliferation (Figure 5E, Supporting Information). On the other hand, no expression of $\alpha$-SMA was detected in the CD90 positive hcMSCs (Figure 5F, Supporting Information), indicating that the human corneal mesenchymal stem cells had not transdifferentiated into smooth muscle-like cells.

### 2.6. Retention of Light-Curable COMatrix in a Human Corneal Stromal Defect Ex Vivo

To explore the retention of LC-COMatrix applied for repair of the corneal stroma, cadaveric human corneas with stromal defects were utilized. As presented in Figure 5A, an anterior lamellar cut with a diameter of 10 mm and thickness of 300 µm was made in cadaveric human corneas and the anterior flap was removed. Then, the created corneal stromal defect was repaired with 2× LC-COMatrix and cured with green light for 4 min. The repaired corneas were placed in standard corneal tissue containers and rotationally shook at 37 °C while a thin layer of corneal preservative solution flowed over the repaired area (Figure S5, Supporting Information). The repaired corneas were followed up with slit-lamp biomicroscopy, optical coherence tomography (OCT), and pachymetry to track the transparency, structure, and thickness map of the repaired human corneas, respectively. As presented in Figure 5B, LC-COMatrix consistently repaired the human corneal stromal defect with a smooth surface with a comparable transparency to native human corneas. During the 30-day incubation of the repaired corneas under constant flow of corneal preservative solution, no sign of detachment was observed on OCT imaging. Moreover, the thickness of the repaired corneas remained stable for 30 days as evident by the results of pachymetry (Figure 5B). On the other hand, the follow up of human corneas with lamellar stromal defects repaired with fibrin glue showed that the fibrin glue had degraded by day 15 (Figure S6, Supporting Information). In the corneal defects repaired with 20% GelMA, the gels had contracted to the center of the corneal stromal defect during follow-up (Figure S6, Supporting Information). Another observed difference between 2× LC-COMatrix and 20% GelMA on OCT imaging was the similarity of LC-COMatrix to human cornea in terms of its optical reflectivity, in contrast to GelMA which demonstrated a significant difference with native corneal tissue (Figure 5; Figure S6, Supporting Information). These observations suggest greater resemblance of LC-COMatrix to native corneal tissue compared to GelMA.

### 2.7. Repair of Rabbit Corneal Stromal Defect by Light-Curable COMatrix

An in vivo rabbit corneal stromal defect was created with a 3 mm lamellar keratectomy technique (illustrated in **Figure 6**A, $N = 4$). The partial thickness stromal defect was then filled with LC-COMatrix, covered with a contact lens to make the hydrogel even with the surrounding corneal tissue, followed by curing with green light (Video S10, Supporting Information). As presented in Figure 6B, the slit lamp biomicroscopy and fluorescent staining showed rapid recovery and closure of corneal epithelium over the applied LC-COMatrix with remarkable transparency of the repaired area during the 28 days follow-up. The OCT imaging during the follow-ups showed full thickness repair of corneal stroma with progressive improvement in the congruency between the repaired area and the surrounding native cornea tissue (Figure 6C). Comparing the thickness (pachymetry) measurements of the cornea immediately after creating the defect (day 0) to the thickness on day 28 showed substantial repair (restored thickness) of the corneal stroma by LC-COMatrix (Figure 6D). The central corneal thickness (CCT) at last follow-up (day 28) was 397 ± 12 µm, which had no statistically significant difference with same

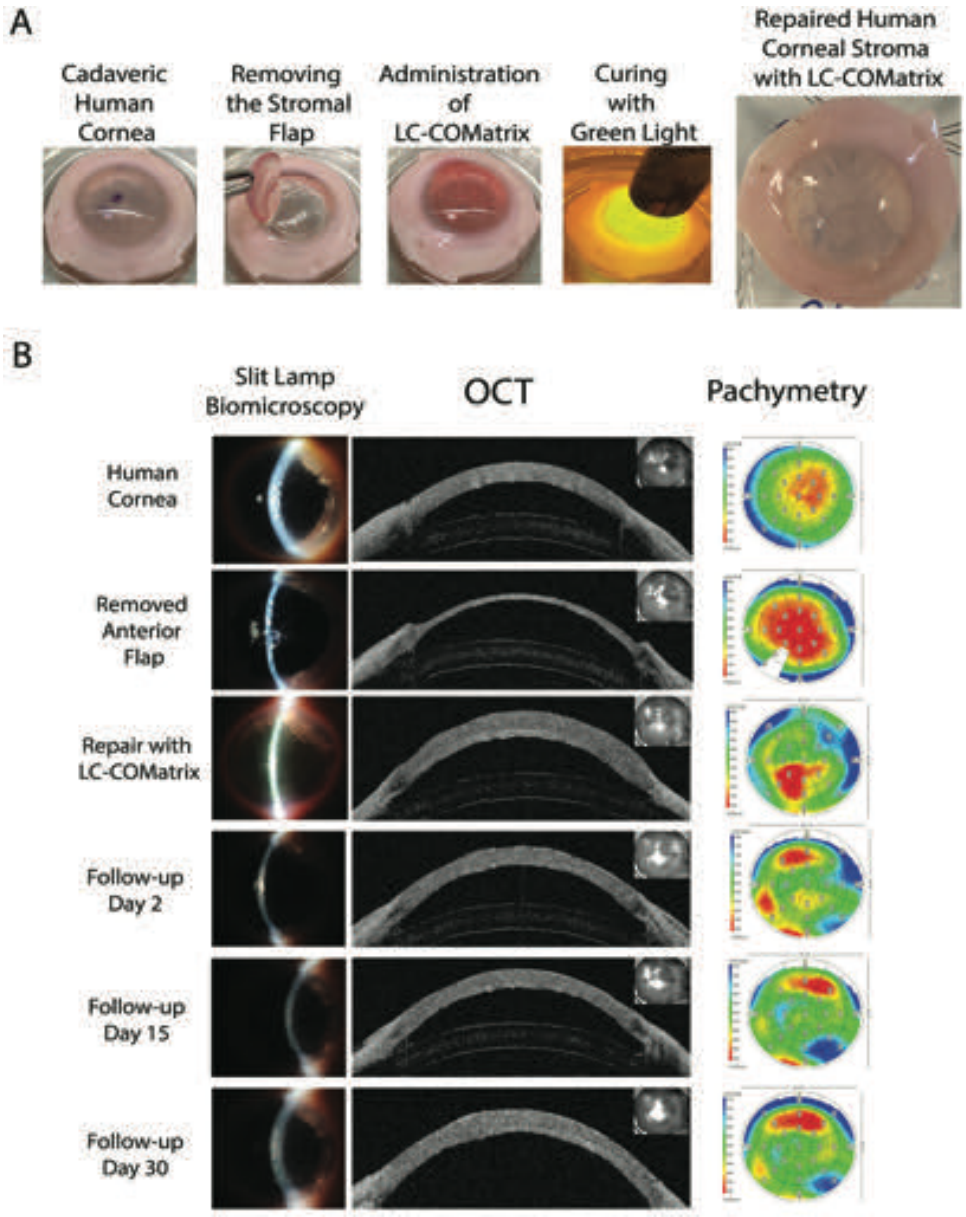


**Figure 5.** Ex vivo repair of human corneal stroma with LC-COMatrix and evaluation of the hydrogel retention. A) The procedure of repairing corneal stromal lamellar defects with 2× LC-COMatrix. B) Slit-lamp biomicroscopy, OCT, and pachymetry of cadaveric human corneas repaired with 2× LC-COMatrix and incubated at 37 °C with orbital shaking followed for 30 days.

corneas' CCTs before performing the surgery (399 ± 8 µm, $N = 4$, Figure S7, Supporting Information). The results of examination of each rabbit are presented in Table S1 of the Supporting Information.

### 2.8. Repair of Corneal Perforation in Rabbit Eyes Using LC-COMatrix In Vivo

An in vivo rabbit corneal macroperforation model was created to assess the potential of LC-COMatrix for repairing corneal full thickness defects. As illustrated in **Figure 7**A and in Video S11 (Supporting Information), a partial (≈50–60%) thickness layer of the rabbit cornea was removed by a 3 mm diameter lamellar keratectomy. A full-thickness cut was then made in the center of the stromal defect using a 1 mm dermal punch and the tissue was removed ($N = 4$). LC-COMatrix was applied to the stromal defect area followed by green-light curing (Video S11, Supporting Information). The administered LC-COMatrix formed strong adhesion to the cornea defect and terminated the leakage of the anterior chamber fluid.

As shown in Figure 7B, after creating the perforation, the anterior chamber collapsed due to leakage of fluid and the iris and lens were found to be touching the cornea. Following closure of the corneal perforation with LC-COMatrix, the anterior chamber deepened at all follow-ups (Figure 7C).

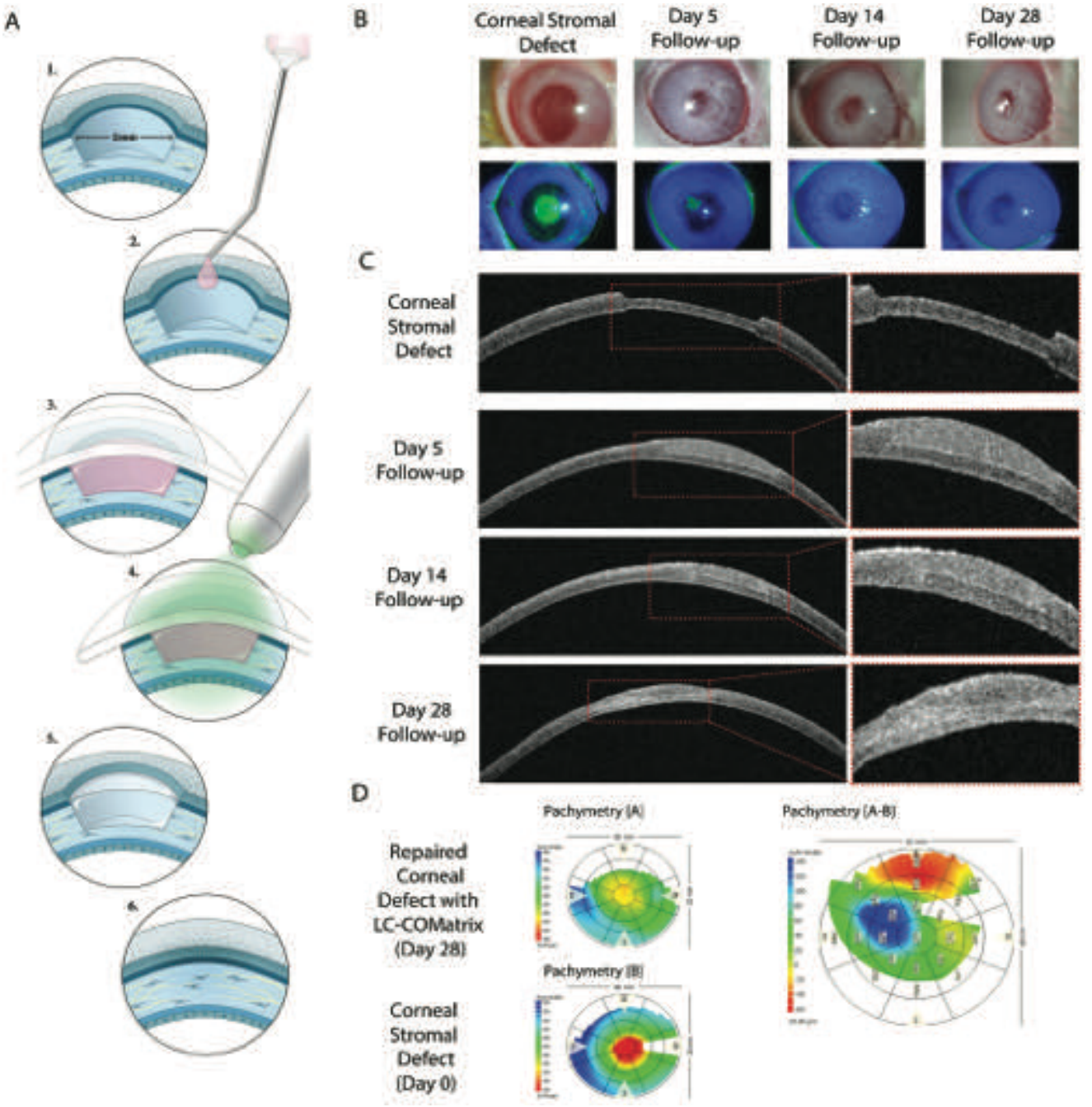


**Figure 6.** In vivo repair of rabbit corneal stromal defect with LC-COMatrix hydrogel. A) Illustration of performed procedures to create a corneal lamellar defect model in rabbit eyes and its repair with 2× LC-COMatrix. B) Slit-lamp microscopy and fluorescein staining of rabbit corneas with lamellar stromal defect repaired with LC-COMatrix during the follow-up. C) OCT imaging of the same corneal defect model repaired with LC-COMatrix during the follow-up. D) Pachymetry difference map showing the filling of the corneal stromal defect with LC-COMatrix.

Part of the iris remained adherent to the repaired area in three rabbits and was fully detached in the other one. The corneal epithelium healed over the defect area after about a week as no fluorescein staining was observed at day 14 of follow-up. The intraocular pressure (IOP) in the surgical eyes had no significant difference with the fellow eye during the follow-up (Figure 7D). Moreover, the CCT at last follow-up (day 28) was 447 ± 12 µm, which is significantly higher than CCT of the same corneas before performing the surgery (396 ± 11 µm, $N = 4$, $p < 0.0001$, Figure S7, Supporting Information). The observed difference is due to administration of higher amount of LC-COMatrix to repair the macroperforation compared to the amount applied for repair of stromal defect to ensure efficient sealing of the perforation. The results of examination of each rabbit are presented in Table S1 of the Supporting Information.

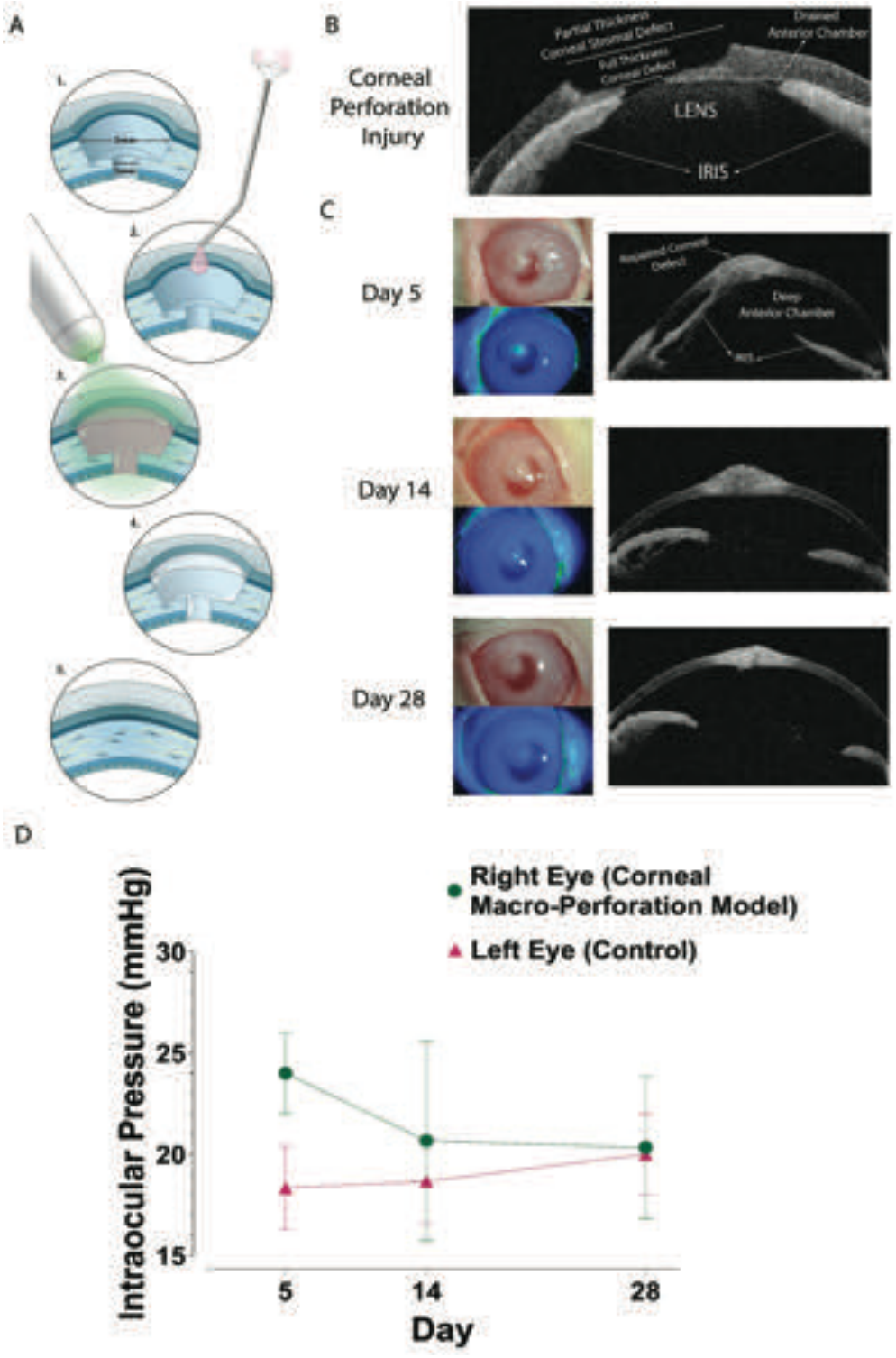


**Figure 7.** In vivo repair of rabbit corneal macroperforation with LC-COMatrix hydrogel. A) Illustration of performed procedures to create a corneal macroperforation model in rabbit eyes and repair with 2× LC-COMatrix. B) OCT of the corneal full-thickness macroperforation model. C) The 28 days' follow-up images (slit lamp biomicroscopy, fluorescein staining, and OCT) of corneal macroperforation model repaired with LC-COMatrix. D) Intraocular pressure of the LC-COMatrix repaired macroperforated eye compared to the normal fellow eye during the follow-up ($N = 4$).

### 2.9. Histological Evaluation and Immunostaining of Repaired Rabbit Corneas

Histology of the repaired rabbit corneas showed some differences between the macroperforation model and the corneal stromal defect model. Specifically, the stromal architecture at the site of repair was lamellar in the perforation model, similar to the control cornea (**Figure 8**A) while it was less lamellar in the corneal stromal defect model at day 28 of follow up. This is the first study reporting the histological characteristics of a repaired corneal macroperforation with a novel light-curable bioadhesive. In both models the corneal epithelium regrew over the repaired area and looked similar to the native control corneal epithelium (Figure 8A). Immunofluorescent staining with the differentiation and stratification marker of corneal epithelial cells, CK-12,[21] revealed that the regrown corneal epithelium on the surface of the repaired area with LC-COMatrix (the applied LC-COMatrix has weak autofluorescence marked with orange stars in Figure 8B) was multilayered and fully differentiated and stratified toward mature corneal epithelial cells in the superficial layers (orange arrows in Figure 8B).

The keratocyte marker, KERA (keratocan), is expressed in the stromal cells in native cornea (orange arrows in Figure 8A top pane). This marker was highly positive in the middle of the repaired area (like a strip) in the macroperforation model (orange stars in Figure 8C middle pane), while the native KERA positive cells under the KERA-positive strip (orange arrows in Figure 8C middle pane). $\alpha$-SMA ($\alpha$-smooth muscle actin) had the same pattern of expression as KERA, like a strip in the repaired macroperforated corneas consistent with a scar-like appearance (orange stars in Figure 8D middle pane). A remodeled native-like corneal stroma is observable on top of the KERA and $\alpha$-SMA positive areas, hashtag (#) markers in Figure 8C,D, middle panes.

KERA positive cells (orange arrows in Figure 8C bottom pane) are present close to the applied LC-COMatrix (orange stars in Figure 8C bottom pane) in repaired corneal stromal defect. The expression of $\alpha$-SMA in repaired partial-thickness corneal stromal defects is similar to control native cornea, indicating that LC-COMatrix did not induce any further transdifferentiation of keratocytes to myofibroblast-like cells.

## 3. Discussion

Novel therapeutic approaches are emerging to overcome the issue of donor cornea shortage, such as keratoprosthetics (artificial cornea)[22] and other collagen-based constructs.[23] Most studies have focused on mimicking the unique characteristics of corneal tissue such as transparency and distinctive biomechanical properties by using natural biomaterials such as combinations of collagens, gelatin, chitosan, and/or alginate.[24] In addition to a corneal stromal substitute, there is a need for a robust tissue-incorporating bioadhesive for closing and repairing corneal defects and macroperforations following severe injuries or infectious/inflammatory diseases. The significance of such a tissue-incorporating bioadhesive is more highlighted in underserved areas and battlefields where advanced surgical infrastructures are not available; and the injured eye must be stabilized to prevent permanent blindness due to tissue necrosis or severe infections (e.g., endophthalmitis).

The goal of this study was to develop and characterize a modified version of a previously reported thermoresponsive COMatrix hydrogel from decellularized porcine corneas.[13,15] The novel modification of COMatrix hydrogel has several advantages over chemical cross-linking methods, which include maintaining the natural corneal composition, with improved biophysical characteristics such as easy handling and administration, fast controllable in situ cross-linking, malleability, and significantly enhanced mechanical stability. The light-curable form of COMatrix has the potential to be administrated as an in situ corneal stromal regenerative material in addition to application as a bioadhesive for closing and repairing corneal macroperforations or incisions following surgeries and trauma. LC-COMatrix has a suitable consistency (e.g., viscosity) for application to the defect area without unnecessary spreading to surrounding areas. Following application, LC-COMatrix can be cured with a green light source such as a battery powered LED or the standard green light filter present on most slit-lamp biomicroscopes. This composition has a similar mechanism of polymerization (visible light curing) with GelMA, a recently introduced bioadhesive for corneal repair.[7] The reported adhesiveness parameters in this study for 20% GelMA (4 min light-curing) are 225.8 ± 32.3 mmHg for ex vivo burst pressure on porcine corneas' substrates and 90.4 ± 10.2 kPa for adhesion strength on porcine skins' substrates. More recently, another type of light-curable gelatin has been fabricated by grafting glycidyl methacrylate on the gelatin with improved adhesiveness properties compared to GelMA.[25] Here we showed superiority of LC-COMatrix in terms of adhesiveness properties compared to GelMA. However, the discrepancies with other reports are potentially related to several different parameters in fabrication and formulation of bioadhesives and settings of performed tests. In terms of formulation, LC-COMatrix has been fabricated by decellularization and processing of porcine corneas by preserving the collagens and sGAGs to represent the natural cornea ECM; however, GelMA is a collagen-only material which is usually derived from porcine skin that is not representative of corneal macromolecular structure. We have previously shown with proteomic analyses that COMatrix is composed of ECM regulatory proteins such as keratocan and lumican which can potentially promote regeneration of the cornea.[13a]

Current commercially available products such as fibrin sealants (e.g., VISTASEAL, TISSEEL), and PEG-based bioglues (ReSure, OcuSeal) need extensive preapplication preparation, which includes thawing, dissolving, and mixing. Moreover, the cross-linking reaction of these products is not controllable. By contrast, LC-COMatrix does not require any preapplication preparation. It is a ready-to-apply syringe like ViscoElastic products that does not require preapplication warming or mixing and it can be applied in a wide range of temperatures in emergency situations. Following application LC-COMatrix can be further manipulated before light-curing (e.g., to make the surface more even with the surrounding tissues) while the cross-linking reaction can be controlled by the intensity and duration of light-curing. In addition, LC-COMatrix has a favorable consistency and can be applied in upright patients (behind slit lamp) without spilling or running off.

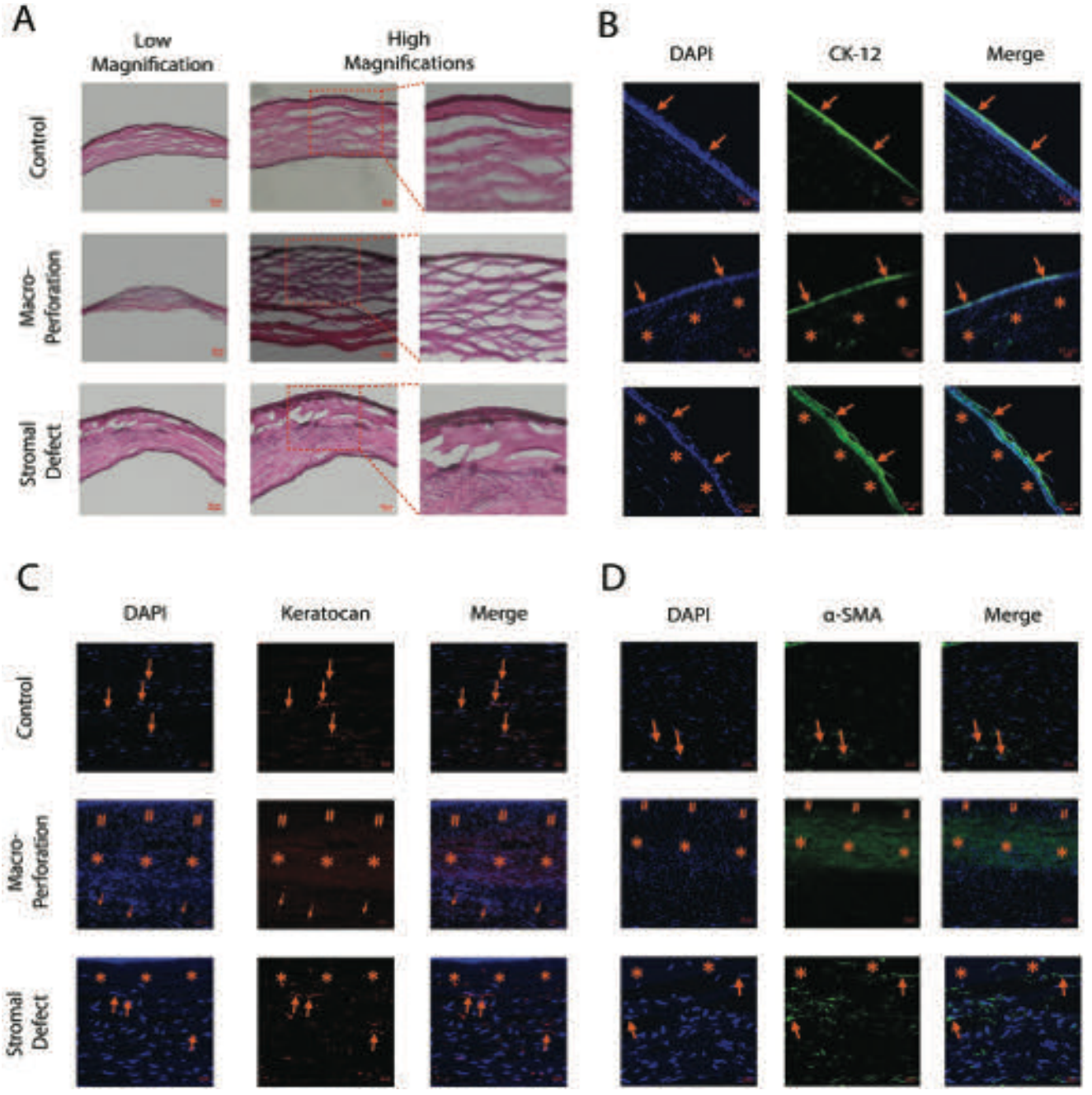


**Figure 8.** Histological and immunofluorescent evaluation of repaired rabbit corneas. A) H&E staining of repaired rabbit corneal macroperforation and stromal defect models compared to control at day 28 of follow-up. The regenerated epithelium on top of the applied LC-COMatrix is similar to native epithelium in native control corneal tissues. B) Anti-cytokeratin-12 (CK-12) staining of repaired rabbit corneas shows complete regeneration and stratification of corneal epithelium on the repaired area with LC-COMatrix in both macroperforation and corneal stromal defect models. The orange arrows point to CK-12 positive epithelium and the orange stars (*) indicate the applied LC-COMatrix with weak autofluorescence C) Antikeratocan staining of tissue samples show keratocan positive cells (keratocytes) in native control corneal stroma (orange arrows). In the repaired macroperforation corneas abundant number of keratocytes are present in the repaired area. The orange stars (*) and hashtags (#) indicate the area that the LC-Comatrix was applied. The hashtags' areas are fully remodeled stroma and the stars' areas are LC-COMatrix with high migration of cells (through iris blood vessels and anterior chamber fluid). Keratocan positive cells (orange arrows) are also present below the strip of highly keratocan positive cells as the native corneal keratocytes. In the repaired corneal stromal defect, the keratocan positive cells (orange arrows) are present near the applied LC-COMatrix (orange stars). D) Anti-$\alpha$-SMA staining of repaired rabbit corneas. $\alpha$-SMA positive cells are pointed by orange arrows. Very few $\alpha$-SMA positive cells are present in native cornea. A strip of $\alpha$-SMA positive staining is present in repaired macroperforation sample (orange stars, *) which is the same pattern as keratocan positive area indicating the differentiation of keratocytes to smooth-muscle like fibroblasts, probably owing to rapid remodeling of the corneal stroma by migrated cells. Orange hashtags (#) are indicating fully remodeled LC-COMatrix. However, the repaired area in stromal defect model is similar to control corneal tissue in terms of expression of $\alpha$-SMA (orange arrows pointing to $\alpha$-SMA positive cells, orange stars (*) indicate applied cell-free LC-COMatrix.

In addition to GelMA,[7,19a] a fibrin-based biomaterial has been introduced for in situ repair of corneal stromal defects.[9a] Like GelMA, this fibrin-based product needs preapplication warming and requires mixing of the prepolymer with cross-linker prior to application. Moreover, it has a very low viscosity (31.7 ± 27.6 Pa s) and would not be suitable for superficial applications or in patients who are upright (similar to GelMA, Figure 3). The measured burst pressure of this product using a porcine cornea as the substrate is 170 ± 16.9 mmHg which is considerably lower than reported burst pressure of LC-COMatrix. Griffith and co-workers repaired an in vivo corneal perforation in a model similar to that in this study using a fibrin-based product which required multiple applications.[9a] By contrast, LC-COMatrix had to be applied only once, and no secondary repair was required. From follow-up of both corneal perforations repaired by the fibrin-based product by Griffith and co-workers and LC-COMatrix, the repaired area became opaque (Figure 7B). However, this study is the first study presenting the histological evaluation of repaired macroperforation by a light-curable bioadhesive. We believe that the reason for low transparency of the closed/repaired areas may be due to invasion of blood vessels from the attached iris and also direct contact with the aqueous humor, which in turn promotes inflammation and development of myofibroblast-like cells (Figure 8D). Additional studies with longer follow-up are needed to determine if there is late remodeling which can reduce the opacity (since a native-like corneal stroma is observable on top of the $\alpha$-SMA positive area, hashtag (#) markers in Figure 8C,D, middle panes) or whether its development can be mitigated, for instance, by limiting the extent of inflammation with corticosteroids. Moreover, since LC-COMatrix can potentially enter the anterior chamber when repairing full thickness perforations, it is necessary in future studies to assess its cytocompatibility with human corneal endothelial cells.

Keratocytes mediate the regeneration of corneal stroma by producing extracellular matrix elements. In the corneal lamellar keratectomy model, the central aspect of the applied LC-COMatrix was not invaded by a high number of keratocytes and they were observed primarily near the edge of the repaired defect (Figure 8C). Future long-term studies of corneal stromal repair by LC-COMatrix are likewise necessary to evaluate the migration and remodeling of the repaired stroma. Overall, the lack of significant inflammation and myofibroblast formation in the nonpenetrating stromal defect model, supports the biocompatibility of LC-COMatrix.

Finally, the COMatrix presented in this study is a xenogeneic product which raises concerns regarding disease transfer from animals to human recipients. Few porcine derived products have been successfully translated into clinical practice or are under evaluation in clinical trials. Pig-derived cardiac valves have been successfully translated into clinical practice.[26] Moreover, a hydrogel fabricated from porcine heart is under investigation in clinical trial phase I/II and promising safety and efficacy was reported.[27] Removing the galactose-$\alpha$1, 3-galactose ($\alpha$-Gal) and *N*-glycolylneuraminic acid (NeuGc) epitopes reduce the risk of immunologic response in recipients, which should be addressed before translation of this product into clinical experiments. Previous studies have shown remarkable efficiency of decellularization methods for removing alpha-gal epitope, which could be improved by using alpha-galactosidase enzyme.[28] Moreover, recent advances in developing genetically modified pigs lacking both $\alpha$-Gal and NeuGc have paved the way for whole organ transplantation and likewise fabrication of products from decellularized extracellular matrix.[29]

## 4. Conclusion

All in all, LC-COMatrix not only compares well to the other state of the art products but also has superior advantages including natural corneal tissue representativeness, user-friendly preparation and application, and nontemperature dependent stable viscosity. Therefore, it has great potential for future modifications and expansion of its applications in ocular surgeries, cell and drug delivery, tissue engineering, and 3D bioprinting.

## 5. Experimental Section

*Fabrication of Light-Curable Porcine Cornea Extracellular Matrix Hydrogel (Light Curable-COMatrix): Harvesting and Decellularization of Porcine Corneas*: Porcine eyeballs were obtained from a certified abattoir (Park Packing CO, Chicago) and transferred to the lab on ice. The eyeballs were then soaked in PBS containing 2% gentamicin and the corneas were excised. The harvested corneas were cut into 2 × 2 mm pieces and washed with PBS and sterile water. Then, the porcine cornea tissue fragments were transferred to a 50 mL conical tube containing 35 mL of 10 × $10^{-3}$ M Tris-HCl contained protease inhibitor cocktail per manufacturer recommended concentration (cOmplete, EDTA-free Protease Inhibitor Cocktail, Roche). After that, the tube underwent 9 cycles of freeze (–80 °C)–thaw (37 °C) in 9 days (1 cycle per day). After freeze–thawing the tissue fragments were washed with pure water and then incubated in DNAse (50 × $10^{-3}$ M Tris-HCl containing 7.5 U $mL^{-1}$ deoxyribonuclease (Sigma, USA)) cocktail for 16 h at 37 °C. The bioburden of the decellularized porcine corneas was then decreased by stirring in 4% ethanol and 0.1% per-acetic acid in pure water for 20 h. The tissues pieces were washed for another 48 h in pure water and then lyophilized for 3 days. The lyophilized decellularized porcine corneas were kept at –80 °C for no more than a month before next step.

*Cryopulverization and Digestion of Decellularized Porcine Corneas*: The lyophilized and decellularized porcine cornea tissue pieces were cryopulverized using Spex 6700 freezer-mill. The pulverized tissue was then digested with pepsin/HCl by ratio of 20 mg decellularized ECM to 1 mg >400 U pepsin in 0.1 M HCl for 72 h at room temperature. At the end of digestion when no more tissue particle was detectable, the solution was neutralized to pH of 7.5 with NaOH and 10× PBS. By neutralization of the solution pH, the pepsin enzyme is deactivated.[30] The result of this step is a thermoresponsive hydrogel, COMatrix hydrogel, which has thermogelation properties at 37 °C.[13]

*Functionalization of Decellularized and Digested Porcine Corneas*: The thermoresponsive COMatrix was reacted with MA with different w/w ratios (2:1, "0.5×", 1:1, "1×", and 1:2, "2×"). The MA was added dropwise and the pH was adjusted to 7.5. The reaction was accomplished at 4 °C for 12 h. Then, the solution was five times diluted with PBS and dialyzed against deionized water for 4 days using 12–14 MWCo dialysis tubes (Sigma). At the end of dialysis, the samples were snap-frozen in liquid nitrogen and lyophilized for 3 days.

*Fabrication of Light-Curable COMatrix Hydrogel*: To formulate the light-curable COMatrix hydrogel, a visible light photoinitiating system was used. The photoinitiating cocktail was prepared by dissolving Eosin Y (0.1 × $10^{-3}$ M final concentration), TEOA (0.75% w/v final concentration), and VC (0.5% w/v final concentration) in 1× PBS. The functionalized COMatrices with different ratios (0.5×, 1×, and 2×) were then dissolved in photoinitiating cocktail (25 mg $mL^{-1}$) to make the ready-to-cure

light-curable (LC)-COMatrix. The prepared LC-COMatrices were then loaded in 1 mL syringes with luer-locks and stored at 4 °C for future experiments no more than two weeks. To apply the LC-COMatrices, a 22-gauge angled cannula was used. Light curing was performed using a custom-made light source fabricated by green LEDs (520 nm, 30° Beam angel) with emission of 100 μW $cm^{-2}$ (Figure S1, Supporting Information). It was found that 4 min green light-curing provided an optimal cross-linked LC-COMatrix. The GelMA hydrogel was fabricated as previously reported.[7,31] 20% (w/v) GelMA combined with the same concentration of photoinitiating cocktail to LC-COMatrix mixture was utilized for perfumed experiments.

*Characterization of Light-Curable COMatrix Hydrogel: Compositional Characterization*: The collagen and sGAG composition of the fabricated light-curable and thermoresponsive COMatrices, GelMA, and human corneas (Eversight, IL, USA) were measured using previously described methods.[13a]

*Measuring the Degree of Functionalization*: To confirm the derivatization of the methacrylate groups and to measure the DoF in fabricated 0.5×, 1×, and 2× LC-COMatrices, 1H NMR, and fluoraldehyde assay were used as previously reported.[32]

Standard proton NMR techniques were utilized to confirm the conjugation of the methacrylate to the COMatrix molecules. Similar concentrations of 0.5×, 1×, and 2× LC-COMatrix and COMatrix samples (0.5 mg $mL^{-1}$) from the same batches were used. All experiments were conducted at 298 K on a Bruker 600 MHz AVANCE III NMR spectrometer operating with a 5 mm D-CH cryogenic probe equipped with a *z*-axis pulsed field gradient. 1D proton spectra were acquired using the standard 1D version of the NOESY experiment with presaturation of water using a total of 512 scans, a sweep width of 16 ppm, acquisition time of 2 s, and a 10 s relaxation delay. Calibration of the proton 90° pulse was verified by null signal of a 360° pulse. Spectra were processed with manual phasing and peak integration.

To measure the DoF of 0.5×, 1×, and 2× LC-COMatrices using the fluoraldehyde assay, the COMatrices from the same batch were used to draw the standard curve. In brief, the LC-COMatrices ($N$ = 4) were dissolved in PBS (0.5 mg $mL^{-1}$) and the same batch of COMatrices were dissolved in PBS (0.05, 0.1, 0.5, 1, and 2 mg $mL^{-1}$). Then, 300 μL of each samples and PBS (control) were mixed with 600 μL of room temperature fluoraldehyde reagent solution (Sigma) for 1 min. After that, 250 μL of each mixture was loaded triplicate in an opaque 96-well plate and the fluorescence intensities were measured at 450 nm with excitation at 360 nm. At the end, the average intensity of PBS was deducted from average intensity of LC-COMatrix and COMatrix (standard) samples. The linear calibration curved was drawn using the COMatrix fluorescence intensities and the DoFs for 0.5×, 1×, and 2× LC-COMatrices were calculated using the standard curve.

*Dry Weight and Swelling Behavior of Light-Curable COMatrix*: To create round disc-shaped constructs, 80 μL of COMatrix or 0.5×, 1× or 2× LC-COMatrix, or 20% GelMA was loaded in a 7 mm diameter PTFE ring (520 μm thickness). The COMatrix samples was incubated at 37 °C for 30 min to set as a gel, while the light curable COMatrices and 20% GelMA were cured with green light for 4 min. Same amount of fibrin glue (prepared based on the manufacturer instructions, TISSEEL Fibrin Sealant, Baxter) was loaded into the ring and incubated at 37 °C for 30 min for full reaction. Cadaveric human corneas (Eversight, Illinois, https://www.eversightvision.org/) with average thickness of 500 to 550 μm were also cut with a 7 mm diameter trephine. All samples were first washed briefly with PBS, weighted (W0) and then put in 500 μL PBS and incubated at 37 °C. The weight of samples was followed at days 1 (W1), 7 (W7), and 18 (W18) after wiping the outside solution using a kimwipe (KIMTECH). At the end of follow-up, all samples were incubated in an oven at 90 °C for 3 h until fully dry and then weighted to measure the dry weight (DW) of each sample. The water content (%) of each sample ($N$ = 3) at each day was then calculated by using the weight at each day of follow-up (Wd) and the following equation

$$Water\ content\ (\%) = \frac{Wd - DW}{Wd} \times 100 \quad (1)$$

The change in water content in each day was then plotted to map the swelling behavior.

*Enzymatic Degradation of Light-Curable COMatrix*: To track the degradation of LC-COMatrix compared to COMatrix, fibrin glue, 20% GelMA, and human cornea with collagenase, the samples were molded and prepared as explained above. Then each sample ($N$ = 3) was incubated in 200 μL of bacterial collagenase type 1 (Sigma, 5 U $mL^{-1}$ in $50 \times 10^{-3}$ M TES and $0.36 \times 10^{-3}$ M calcium chloride), as the common protocol to assess the degradability of a developed biomaterial for cornea regeneration.[33] Each sample was weighted on days 0, 1, 2, 5, and 10 and the weight change (%) was calculated.

*Evaluating Displacement of LC-COMatrix by Gravity*: To evaluate the effect of gravity on spreading of the LC-COMatrix, a gravity displacement test was performed. The 2× LC-COMatrix, ophthalmic viscoelastic, fibrin glue, 20% GelMA, and cyanoacrylate were applied on an upright cadaveric human cornea mounted on a slit-lamp (to simulate the same condition to apply the bioadhesive on a patient cornea in clinic). Video recording was performed from administration of the samples (0 s) to 5 min later (300 s). Moreover, the covered area with each bioadhesive immediately after administration and after 5 min was measured by image analysis ($N$ = 3) using ImageJ software (National Institutes of Health, Bethesda, MD, https://imagej.nih.gov/ij/). The change in the covered area (%) was calculated using the following formula

$$\text{Change in covered area}\,(\%) = \left(\frac{\text{covered area After 5 minutes} - \text{covered area immidiately after administration}}{\text{covered area immidiately after administration}}\right) \times 100 \quad (2)$$

*Rheological Characterization and Viscosity Measurement of LC-COMatrix*: To measure the viscosity of 2× LC-COMatrix and 20% GelMA, the hydrogel was loaded in a rotational rheometer (Kinexus Ultra+, Malvern) with a parallel 25 mm plate and temperature controller. The gap was set to 0.4 mm and the viscosity (PaS) was recorded with shear rate change from 0.01 to 1000 (S-1) at different temperatures (12, 25, and 37 °C). The same recording setting was used for fibrin glue (TISSEEL) and Ophthalmic ViscoElastic Agent (sodium chondroitin sulfate/sodium hyaluronate ophthalmic, Alcon Laboratories, Inc). The recorded viscosities were plotted against shear rate.

*Rheological Photogelation Kinetics and Characterization of LC-COMatrix*: The 0.5×, 1×, and 2× LC-COMatrices and 20% GelMA were loaded on a quartz bed of a rotational rheometer (Kinexus Ultra+, Malvern) with a parallel 25 mm plate and a custom-made green light source. The gap was adjusted to 0.4 mm and the shear moduli (storage, $G'$ and loss, $G''$) were recorded with a frequency of 0.159 Hz and strain of 5%. After 1 min of recording the green light was turned on while recording continued and later the light was turned off at minute 5. The recording was continued for another 5 min. All the above tests were also performed on fibrin glue prepared per manufacturer instructions and incubated for 30 min for full reaction.

*Ex Vivo Bioadhesion Strength Measurements*: The bioadhesion strength of 0.5×, 1×, and 2× COMatrices and 20% GelMA were measured using fresh cadaveric human corneas as substrate (Eversight, Illinois, https://www.eversightvision.org/).[34] The human corneas (average thickness of 500 μm) were cut using a 10 mm trephine and then cut into two halves. Each half was loaded on an already half-cut contact lens holder to preserve the cornea curvature. As illustrated in Figure 4A, 2 mm of half-corneas was in touch with half-contact lens holder secured with cyanoacrylate glue (Krazy Glue, Elmer's Products Inc., Columbus, OH). The contact lens holder was secured in grips of a mechanical testing machine (225lbs Actuator equipped with a 5 N load cell, TestResources) and aligned with a 1 mm gap. Then, the LC-COMatrices were loaded in between the half-corneas with a length of 3 mm and thickness of 0.5 mm using a 22-gauge angled cannula. After that, the LC-COMatrices and 20% GelMA were cured with a green-light source for 4 min. The

tensile test was run at the rate of 1 mm $min^{-1}$ and the adhesion strength (MPa) was calculated using the highest recorded load (N) divided by the surface area (3 mm × 0.5 mm).

*Ex Vivo Burst Pressure Measurements*: The ex vivo sealing capabilities of the 05×, 1×, and 2×, LC-COMatrices, and 20% GelMA were evaluated using a burst pressure measurement setup. The fresh cadaveric human corneas (Eversight, Illinois, https://www.eversightvision.org/) were loaded in an artificial anterior chamber (CORONET) connected to a same-level pressure sensor and pump. Four different types of controlled corneal injuries were created on the cadaveric human corneas (at pressure of 18 mmHg) including 1 and 2 mm punch full thickness injury with the cut cornea tissue removed after punching; and, 2.75 and 5.9 mm cut injuries made by 2.75 mm keratome and scalpel (size 11) knives, respectively. After removing the air in the chamber and drying the area of injury, the COMatrices and GelMA were applied using a 22-gauge cannula and cured with green light for 4 min (Figure 4). Then, the pressure was increased by forward movement of the plunger of a 20 mL syringe loaded with blue colored PBS with speed of 1 mL $min^{-1}$ until burst/failure visualized in the video being recorded from top. 2× LC-COMatrix showed the best performance in the characterization and ex vivo experiments; so, it has been used for further in vitro, ex vivo, and in vivo experiments.

*In Vitro Cytocompatibility of Light-Curable COMatrix with Human Corneal Epithelial and Stromal Cells*: Immortalized HCECs were kindly provided by Dr. Deepak Shukla (Illinois Eye and Ear Infirmary, University of Illinois at Chicago).[35] The HCECs were expanded in high-glucose DMEM medium (4500 mg $L^{-1}$, Fisher Scientific, USA) containing 10% FBS (Fisher Scientific, USA) and 1× Antibiotic-Antimycotic (Fisher Scientific, USA) for no more than 40 passages. The human corneal MSCs (hcMSCs) were obtained from cadaveric human corneas as described before by the group.[36] In brief, the centers of cadaveric human corneas (Eversight, Chicago) were cut with 8 mm trephine and the periphery (containing the limbal area) was cut into four pieces. Each piece was then put in a well of 6 well plate until the hcMSCs were outgrow. The outgrown cells (P0) were collected and expanded. hcMSCs with passage 3 and 4 were used for further experiments. The $\alpha$-MEM medium (Fisher Scientific, USA) containing 10% fetal bovine serum (Fisher Scientific, USA) and 1× Antibiotic-Antimycotic (Fisher Scientific, USA) was used in all experiments with hcMSCs.

The cytocompatibility of thermoresponsive COMatrix has been previously shown.[13] In this study, the cell compatibility of 2× Light Curable-COMatrix compared to thermoresponsive COMatrix was evaluated. The cell-free thermogelation was induced as previously described by incubating the tissue culture plate at 37 °C for 30 min (75 µL COMatrix, 25 mg $mL^{-1}$, was loaded in each well of a 48 well plate, $N = 3$). The cell-free photogelation of 2 LC-COMatrix was induced by curing the hydrogel loaded in 48 well plate (25 mg $mL^{-1}$, 75 µL in each well) with green light for 4 min. Then, the HCECs or hcMSCs ($3 \times 10^3$ cells) were seeded on top of the gel formed COMatrices using the above-mentioned media for each cell type (2D cell culture).

For 3D cell culture, the hcMSCs ($3 \times 10^4$ cells) were mixed with 80 µL of 15 mg $mL^{-1}$ 2× LC-COMatrix, loaded in a well of a 48 well plate and cured with green light for 2 min. Then, 300 µL of $\alpha$-MEM media containing 10% FBS and 1× antibiotic was added to each well. The hydrogels were cultured for two weeks.

*Live–Dead and Metabolic Activity Assays*: To monitor the viability and number of 2D seeded HCECs and hcMSCs on COMatrix and LC-COMatrix, live–dead and metabolic activity assays were performed, respectively. On days 1, 4, 9, and 15, the cells were stained with Calcein-AM (live cells), propidium iodide (PI, dead cells), and Hoechst 33342 (total cells, all from Sigma, USA) for 1 h by incubating at 37 °C in humidified atmosphere air with 5% $CO_2$. The cells were imaged using ZEISS Cell Observer SD Spinning Disk Confocal Microscope (Zeiss, Germany). The metabolic activity of cells as representative of cell numbers was also assesses using Cell Counting Kit-8 (CCK-8, Sigma, USA) per the manufacturer's recommendation.

*Immunofluorescence Staining*: The 2× LC-COMatrices combined with hcMSCs cultured for 2 weeks were fixed in 4% paraformaldehyde (PFA) for an overnight and embedded in optimal cutting temperature (O.C.T, TissueTek) and frozen on dry ice. The fixed hydrogels were sectioned by Cryostat (Fisher Scientific, USA) and transferred on a histological slide. The slides were then fixed with 4% PFA for 15 min and washed with PBS. The samples were blocked with 3% bovine serum albumin for an hour and incubated with primary antibodies (anti-CD90, anti-Ki-67, and anti-$\alpha$-SMA) overnight. (The details of all utilized antibodies in this study are available in Table S2, Supporting Information.) Then, the sections were washed with PBS and incubated with secondary antibodies for 1 h at room temperature (Table S2, Supporting Information). After several rounds of washing the slides were mounted with ProLong Gold Antifade Mountant with DAPI (Thermo Fisher Scientific) and visualized with a confocal microscope (LSM 710, Carl Zeiss, Germany). The Images were analyzed with ZEN Lite software (Zeiss, Germany).

*Ex Vivo Retention of Light-Curable COMatrix in Human Corneal Stromal Defect Model*: As shown in Figure 5A, an anterior lamellar cut (10 mm diameter, 300 µm thickness) was made in cadaveric human corneas and the anterior stromal flap was removed. The created defects were then repaired with 2× LC-COMatrix (25 mg $mL^{-1}$) or 20% GelMA and cured with green light for 4 min. The corneas ($N = 3$) were placed in donor cornea holders containing 9 mL of Life4C (donor cornea preservative solution) and put on an orbital shaker upside down (Figure S5, Supporting Information, the corneas were facing up with a layer of solution covering them). After that, the shaker was in a 37 °C incubator starting with 50 orbital shakes per minute. The human corneas were then follow-up with slit-lamp biomicroscopy, OCT and pachymetry to evaluate the adhesiveness/attachment, transparency, morphology, and thickness of the repaired corneas with LC-COMatrix for 30 days. The human corneal stromal defects were also repaired with fibrin glue as control.

*Rabbit Corneal Perforation and Stromal-Defect Models and Repair with Light-Curable COMatrix*: All animal experiments were performed in accordance with guidelines of Association for Research in Vision and Ophthalmology and were approved by the University of Illinois Biologic Resources Laboratory (20-216). All surgeries were performed by the same surgeon (G.Y.). New Zealand rabbits were anesthetized using subcutaneous (SC) injection of ketamine (45 mg $kg^{-1}$) and xylazine (5 mg $kg^{-1}$), and a drop of proparacaine 0.5% was instilled into the right eye. Then, povidone-iodine 1% was applied to the eye and removed after 30 s with a sterile sponge. A sterile drape covered the right eye surrounding area.

To create the partial thickness corneal stromal-defect model ($N = 4$), the anterior lamellar keratectomy was performed by a 3 mm trephination (150–170 µm depth) at the center of cornea followed by performing the lamellar keratectomy using a 1.2 mm angled minicrescent knife (Figure 6A; Video S10, Supporting Information). Then, proper amount (10–20 µL) of the 2× LC-COMatrix preloaded in a syringe (Figure S1, Supporting Information) was applied using a 22-gauge blunt cannula and trimmed. After that, an 8 mm diameter contact lens was fit on the defect area to adjust the hydrogel with surrounding tissues, and the repaired area was cured with visible green light for 4 min. A 14 mm contact lens was applied on the cornea for at least 24 h.

To create the full thickness corneal perforation model ($N = 4$, Figure 7A; Video S11, Supporting Information); first, a partial thickness lamellar keratectomy was performed as explained above. Then, by using a 1 mm punch biopsy, a full thickness cut was performed at the center of the lamellar keratectomy area and the tissue was removed using a minicrescent knife (if needed). After drying the drained fluid from the anterior chamber, the created perforation defect was repaired with 2× LC-COMatrix (20–40 µL, applied using a preloaded syringe with a 22-gauge blunt cannula, Figure S1, Supporting Information) and cured with green-light for 4 min. After assuring no leakage, a 14 mm soft contact lens was placed on the eye and kept for at least 24 h.

The eyes from both corneal injury models were treated with a combination eye drop containing dexamethasone, neomycin, and polymyxin B for 7 days after surgery, two times per day. The follow ups were performed with OCT imaging and pachymetry, slit lamp biomicroscopy and fluorescein staining for 30 days. The IOP of the

eyes (corneal perforation model) was also measured using a handheld Tonometer (iCare Tonometer) during the follow-ups.

*Histological Evaluations and Immunofluorescence Staining*: After humanly euthanizing of the rabbits with pentobarbital overdose (1 mL/10 lbs, IV) under anesthesia (ketamine/xylazine, SC), the corneas were removed and fixed in 4% PFA overnight. Then, the tissues were washed with PBS and dropped in 15% sucrose solution in PBS until they sank and then dropped in 30% sucrose solution in PBS until they sank. After that, the samples were embedded in O.C.T and frozen on dry ice, and sectioned by Cryostat (Fisher Scientific, USA) and transferred on a histological slide for staining. The hematoxylin and eosin staining was performed as described earlier.[13b] The immunofluorescence staining was performed as described above using the primary antibodies summarized in Table S2 of the Supporting Information.

*Statistical Analysis*: Data are shown as mean ± standard deviation (SD). No preprocessing was performed on the collected data. Statistical analyses were done by GraphPad Prism software version 8.3.0 (538) for Windows, (GraphPad Software, San Diego, CA, USA, www.graphpad.com) using Student's *t*-test for comparing the means between two groups and one-way analysis of variance (ANOVA) and Tukey post-test for more than two groups (sample size (N) for each test is mentioned above in this section, in Section 2, and in figure legends. All performed tests were two-sided). *P*-values less than 0.05 were considered as statistically significant difference between groups.

## Supporting Information

Supporting Information is available from the Wiley Online Library or from the author.

## Acknowledgements

The authors want to thank Ruth Zelkha and Michael Sun for their help in performing some experiments. This study is extracted from Ph.D. dissertation of G.Y. A provisional US and international patent has been filed at USPTO on September 2, 2021 by G.Y., A.R.D., and The Office of Technology Management at University of Illinois at Chicago. This work was supported by R01 EY024349 (A.R.D.), R01EY027912 (M.I.R.), and Core Grant for Vision Research EY01792 (M.I.R.) from NEI/NIH, and Unrestricted Grant to the Department and Physician-Scientist Award (A.R.D.) both from Research to Prevent Blindness, and Eversight. The funders had no role in study design, data collection and analysis, decision to publish, or preparation of the manuscript.

## Conflict of Interest

The authors declare no conflict of interest.

## Author Contributions

G.Y. and A.R.D. contributed to conceptualization. G.Y., Y.P., E.A., T.S., M.I.R., and A.R.D. contributed to methodology. G.Y., X.S., T.N., K.N.A., O.J., Y.J., and M.P. carried out investigation. G.Y. carried out visualization. M.I.R. and A.R.D. assisted in supervision. G.Y. wrote and drafted the original manuscript. A.R.D. and E.A. helped in writing, reviewing, and editing the paper.

## Data Availability Statement

The data that support the findings of this study are available from the corresponding author upon reasonable request.

## Keywords

bioadhesives, corneas, decellularized tissues, extracellular matrix, hydrogels, light-curing

Received: December 30, 2021
Revised: February 9, 2022
Published online: March 8, 2022

[1] P. Gain, R. Jullienne, Z. He, M. Aldossary, S. Acquart, F. Cognasse, G. Thuret, *JAMA Ophthalmol.* **2016**, *134*, 167.
[2] a) S. L. Wilson, L. E. Sidney, S. E. Dunphy, J. B. Rose, A. Hopkinson, *J. Funct. Biomater.* **2013**, *4*, 114; b) W. Shi, Q. Zhou, H. Gao, S. Li, M. Dong, T. Wang, Y. Jia, C. Dong, X. Wang, Z. Guo, L. Zhao, X. Hu, L. Xie, *Adv. Funct. Mater.* **2019**, *29*, 1902491.
[3] C. H. Yoon, H. J. Choi, M. K. Kim, *Prog. Retinal Eye Res.* **2021**, *80*, 100876.
[4] G. Trujillo-de Santiago, R. Sharifi, K. Yue, E. S. Sani, S. S. Kashaf, M. M. Alvarez, J. Leijten, A. Khademhosseini, R. Dana, N. Annabi, *Biomaterials* **2019**, *197*, 345.
[5] A. Panda, S. Kumar, A. Kumar, R. Bansal, S. Bhartiya, *Indian J. Ophthalmol.* **2009**, *57*, 371.
[6] D. N. Papadopoulou, A. Sionga, G. Karayannopoulou, K. Natsis, A. Komnenou, G. Mangioris, A. Kalpatsanidis, A. Manthos, N. Georgiadis, V. Karampatakis, *Eur. J. Ophthalmol.* **2013**, *23*, 646.
[7] E. Shirzaei Sani, A. Kheirkhah, D. Rana, Z. Sun, W. Foulsham, A. Sheikhi, A. Khademhosseini, R. Dana, N. Annabi, *Sci. Adv.* **2019**, *5*, 1281.
[8] L. Li, C. Lu, L. Wang, M. Chen, J. White, X. Hao, K. M. McLean, H. Chen, T. C. Hughes, *ACS Appl. Mater. Interfaces* **2018**, *10*, 13283.
[9] a) C. D. McTiernan, F. C. Simpson, M. Haagdorens, C. Samarawickrama, D. Hunter, O. Buznyk, P. Fagerholm, M. K. Ljunggren, P. Lewis, I. Pintelon, D. Olsen, E. Edin, M. Groleau, B. D. Allan, M. Griffith, *Sci. Adv.* **2020**, *6*, 2187; b) B. Ozcelik, K. D. Brown, A. Blencowe, K. Ladewig, G. W. Stevens, J. P. Scheerlinck, K. Abberton, M. Daniell, G. G. Qiao, *Adv. Healthcare Mater.* **2014**, *3*, 1496.
[10] a) M. Ahearne, A. P. Lynch, *Tissue Eng., Part C* **2015**, *21*, 1059; b) H. Kim, M. N. Park, J. Kim, J. Jang, H. K. Kim, D. W. Cho, *J. Tissue Eng.* **2019**, *10*, 204173141882338; c) F. Wang, W. Shi, H. Li, H. Wang, D. Sun, L. Zhao, L. Yang, T. Liu, Q. Zhou, L. Xie, *Ocul. Surf.* **2020**, *18*, 748.
[11] a) L. T. Saldin, M. C. Cramer, S. S. Velankar, L. J. White, S. F. Badylak, *Acta Biomater.* **2017**, *49*, 1; b) J. L. Dziki, D. S. Wang, C. Pineda, B. M. Sicari, T. Rausch, S. F. Badylak, *J. Biomed. Mater. Res., Part A* **2017**, *105*, 138.
[12] R. Sharifi, Y. Yang, Y. Adibnia, C. H. Dohlman, J. Chodosh, M. Gonzalez-Andrades, *Sci. Rep.* **2019**, *9*, 1876.
[13] a) G. Yazdanpanah, Y. Jiang, B. Rabiee, M. Omidi, M. I. Rosenblatt, T. Shokuhfar, Y. Pan, A. Naba, A. R. Djalilian, *Tissue Eng., Part C* **2021**, *27*, 307; b) G. Yazdanpanah, R. Shah, S. R. R. Somala, K. N. Anwar, X. Shen, S. An, M. Omidi, M. I. Rosenblatt, T. Shokuhfar, A. R. Djalilian, *Ocul. Surf.* **2021**, *21*, 27.
[14] S. Zhu, Q. Yuan, M. Yang, J. You, T. Yin, Z. Gu, Y. Hu, S. Xiong, *Mater. Sci. Eng., C* **2019**, *96*, 446.
[15] J. Fernandez-Perez, M. Ahearne, *Sci. Rep.* **2019**, *9*, 14933.
[16] a) R. A. Muzzarelli, M. El Mehtedi, C. Bottegoni, A. Aquili, A. Gigante, *Mar. Drugs* **2015**, *13*, 7314; b) W. E. Hennink, C. F. van Nostrum, *Adv. Drug Delivery Rev.* **2012**, *64*, 223.
[17] B. H. Lee, N. Lum, L. Y. Seow, P. Q. Lim, L. P. Tan, *Materials* **2016**, *9*, 797.
[18] Y. Wu, A. Wenger, H. Golzar, X. S. Tang, *Sci. Rep.* **2020**, *10*, 20648.
[19] a) C. Jumelle, A. Yung, E. S. Sani, Y. Taketani, F. Gantin, L. Bourel, S. Wang, E. Yuksel, S. Seneca, N. Annabi, R. Dana, *Acta*

*Biomater.* **2022**, *137*, 53; b) I. Pepelanova, K. Kruppa, T. Scheper, A. Lavrentieva, *Bioengineering* **2018**, *5*, 55.
[20] S. E. Wilson, *Exp. Eye Res.* **2020**, *201*, 108272.
[21] N. Tanifuji-Terai, K. Terai, Y. Hayashi, T.-i. Chikama, W. W.-Y. Kao, *Invest. Ophthalmol. Visual Sci.* **2006**, *47*, 545.
[22] P. Chhadva, M. S. Cortina, *Curr. Opin. Ophthalmol.* **2019**, *30*, 243.
[23] a) H. Hong, H. Kim, S. J. Han, J. Jang, H. K. Kim, D. W. Cho, D. S. Kim, *Mater. Sci. Eng., C* **2019**, *103*, 109837; b) H. Hong, J. Kim, H. Cho, S. M. Park, M. Jeon, H. K. Kim, D. S. Kim, *Biofabrication* **2020**, *12*, 045030; c) E. Edin, F. Simpson, M. Griffith, *Methods Mol. Biol.* **2020**, *2145*, 169; d) I. Brunette, C. J. Roberts, F. Vidal, M. Harissi-Dagher, J. Lachaine, H. Sheardown, G. M. Durr, S. Proulx, M. Griffith, *Prog. Retinal Eye Res.* **2017**, *59*, 97.
[24] a) J. J. Chae, W. M. Ambrose, F. A. Espinoza, D. G. Mulreany, S. Ng, T. Takezawa, M. M. Trexler, O. D. Schein, R. S. Chuck, J. H. Elisseeff, *Acta Ophthalmol.* **2015**, *93*, 57; b) X. Calderon-Colon, Z. Xia, J. L. Breidenich, D. G. Mulreany, Q. Guo, O. M. Uy, J. E. Tiffany, D. E. Freund, R. L. McCally, O. D. Schein, J. H. Elisseeff, M. M. Trexler, *Biomaterials* **2012**, *33*, 8286; c) M. Banitt, J. B. Malta, H. K. Soong, D. C. Musch, S. I. Mian, *Curr. Eye Res.* **2009**, *34*, 706; d) J. B. Rose, S. Pacelli, A. J. E. Haj, H. S. Dua, A. Hopkinson, L. J. White, F. Rose, *Materials* **2014**, *7*, 3106; e) T. Gratieri, G. M. Gelfuso, E. M. Rocha, V. H. Sarmento, O. de Freitas, R. F. Lopez, *Eur. J. Pharm. Biopharm.* **2010**, *75*, 186.
[25] S. Sharifi, M. M. Islam, H. Sharifi, R. Islam, D. Koza, F. Reyes-Ortega, D. Alba-Molina, P. H. Nilsson, C. H. Dohlman, T. E. Mollnes, J. Chodosh, M. Gonzalez-Andrades, *Bioact. Mater.* **2021**, *6*, 3947.
[26] A. W. Godehardt, R. Ramm, B. Gulich, R. R. Tonjes, A. Hilfiker, *Xenotransplantation* **2020**, *27*, 12565.
[27] J. H. Traverse, T. D. Henry, N. Dib, A. N. Patel, C. Pepine, G. L. Schaer, J. A. DeQuach, A. M. Kinsey, P. Chamberlin, K. L. Christman, *JACC Basic Transl. Sci.* **2019**, *4*, 659.
[28] a) S. Y. Choi, H. J. Jeong, H. G. Lim, S. S. Park, S. H. Kim, Y. J. Kim, *J. Heart Valve Dis.* **2012**, *21*, 387; b) H. W. Gao, S. B. Li, W. Q. Sun, Z. M. Yun, X. Zhang, J. W. Song, S. K. Zhang, L. Leng, S. P. Ji, Y. X. Tan, F. Gong, *Tissue Eng., Part C* **2015**, *21*, 1197; c) M. S. Kim, H. G. Lim, Y. J. Kim, *Eur. J. Cardiothorac. Surg.* **2016**, *49*, 894; d) K. R. Stone, A. Walgenbach, U. Galili, *Tissue Eng., Part B* **2017**, *23*, 412.
[29] D. K. Cooper, B. Ekser, J. Ramsoondar, C. Phelps, D. Ayares, *J. Pathol.* **2016**, *238*, 288.
[30] R. A. Pouliot, B. M. Young, P. A. Link, H. E. Park, A. R. Kahn, K. Shankar, M. B. Schneck, D. J. Weiss, R. L. Heise, *Tissue Eng., Part C* **2020**, *26*, 332.
[31] A. Assmann, A. Vegh, M. Ghasemi-Rad, S. Bagherifard, G. Cheng, E. S. Sani, G. U. Ruiz-Esparza, I. Noshadi, A. D. Lassaletta, S. Gangadharan, A. Tamayol, A. Khademhosseini, N. Annabi, *Biomaterials* **2017**, *140*, 115.
[32] a) B. B. Rothrauff, L. Coluccino, R. Gottardi, L. Ceseracciu, S. Scaglione, L. Goldoni, R. S. Tuan, *J. Tissue Eng. Regener. Med.* **2018**, *12*, 159; b) D. Loessner, C. Meinert, E. Kaemmerer, L. C. Martine, K. Yue, P. A. Levett, T. J. Klein, F. P. Melchels, A. Khademhosseini, D. W. Hutmacher, *Nat. Protoc.* **2016**, *11*, 727.
[33] F. C. Simpson, C. D. McTiernan, M. M. Islam, O. Buznyk, P. N. Lewis, K. M. Meek, M. Haagdorens, C. Audiger, S. Lesage, F. X. Gueriot, I. Brunette, M. C. Robert, D. Olsen, L. Koivusalo, A. Liszka, P. Fagerholm, M. Gonzalez-Andrades, M. Griffith, *Commun. Biol.* **2021**, *4*, 608.
[34] O. Jeon, J. E. Samorezov, E. Alsberg, *Acta Biomater.* **2014**, *10*, 47.
[35] T. Yadavalli, R. Suryawanshi, M. Ali, A. Iqbal, R. Koganti, J. Ames, V. K. Aakalu, D. Shukla, *Ocul. Surf.* **2020**, *18*, 221.
[36] S. Jabbehdari, G. Yazdanpanah, L. N. Kanu, K. N. Anwar, X. Shen, B. Rabiee, I. Putra, M. Eslani, M. I. Rosenblatt, P. Hematti, A. R. Djalilian, *Transl. Vis. Sci. Technol.* **2020**, *9*, 26.